RIKEN Sept., 2007

(expecting experimentalists as an audience)

One-particle motion in nuclear many-body problem

- from spherical to deformed nuclei - from stable to drip-line
- from static to rotating field - from particle to quasiparticle
- collective modes and many-body correlations in terms of one-particle motion

Ikuko Hamamoto

Division of Mathematical Physics, LTH,
University of Lund, Sweden

The figures with figure-numbers but without reference, are taken from

the basic reference : A.Bohr and B.R.Mottelson, Nuclear Structure, Vol. I & II

1. Introduction

Mean-field approximation to many-body system

The study of one-particle motion in the mean field is the basis for understanding not only single-particle mode but also many-body correlation.

Mean field ⟵ Hartree-Fock approximation

Self-consistent potential = Hatree-Fock potential

Phenomenological one-body potential

(convenient for understanding the physics in a simple terminology and in a systematic way)

Harmonic-oscillator potential

Woods-Saxon potential

Note, for example,
the shape of a many-body system can be obtained only from the one-body density

⟵ mean-field approximation

Harmonic-oscillator potential is exclusively used, for example,
the system with a finite number of electrons bound by an external field
(= a kind of NANO structure system).
This system is a sufficiently bound system so that harmonic-oscillator potential is a good approximation to the effective potential.

Another finite system to which quantum mechanics is applied is
clusters of metalic atoms

$\longrightarrow$ shell-structure based on one-particle motion of electrons

In this system a harmonic-oscillator potential is also often used.

2. Mean-field approximation to spherical nuclei

2.1. Phenomenological one-body potentials

3-dimensional harmonic oscillator potential

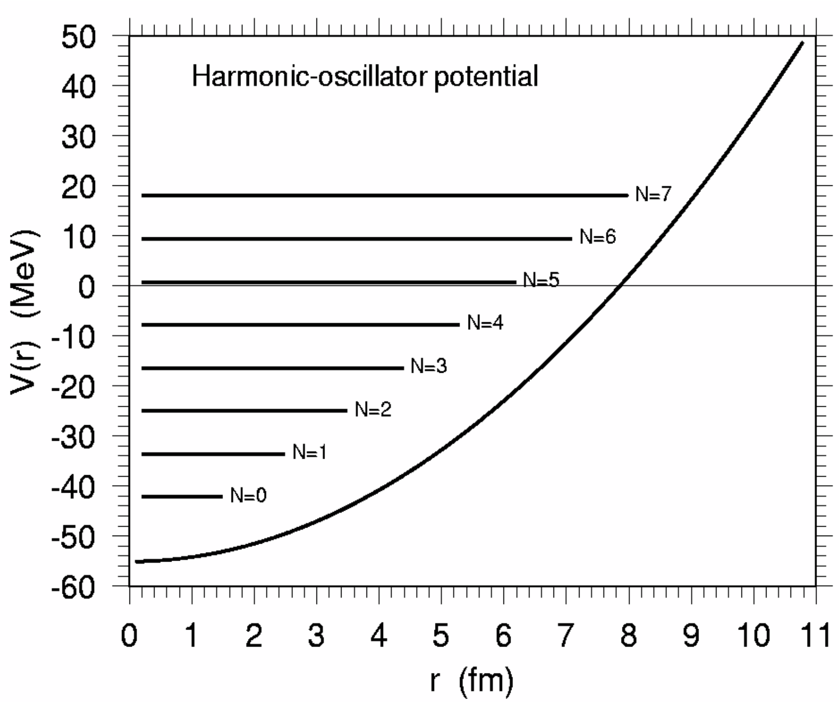

In the above figure

$$V(r) = \frac{1}{2}m\omega^2 r^2 + \underline{const}$$

where const = –55 MeV

$\hbar\omega$ = 8.6 MeV

$$H = -\frac{\hbar^2}{2m}\Delta + \underline{\frac{1}{2}m\omega^2 r^2}$$

harmonic-oscillator potential

has a spectrum

$$\varepsilon = \left(N + \frac{3}{2}\right)\hbar\omega$$

where

$N = n_x + n_y + n_z$ in rectilinear coordinates

$= 2(n_r - 1) + \ell$ in polar coordinates

ℓ = *N, N-2, … 0 or 1*

Degeneracy of the major shell with a given *N*

$\sum_{\ell} 2(2\ell + 1)$ = *(N+1)(N+2)*

spin ↑↓ (ℓ = even for N=even, odd for N=odd)

leads to the magic numbers

2, 8, 20, 40, 70, 112, 168, …

One-particle levels for β stable nuclei

($S_n \approx S_p \approx$ 7-10 MeV)

Modified harmonic-oscillator potential can often be a good approximation.

Large energy gap in one-particle spectra

⟷ Magic number

N, Z = 8, 20,28,50,82,126, …

Nuclei with magic number : spherical shape

Normal-parity orbits ← majority in a major shell of medium-heavy nuclei

High-j orbits, $1g_{9/2}$, $1h_{11/2}$, $1i_{13/2}$, $1j_{15/2}$,
which have parity different from the neighboring orbits do not mix with them under quadrupole ($Y_{2\mu}$) deformation and rotation.

One-particle motion in the mean-field

→ shell structure (= bunching of one-particle levels)

→ nuclear shape

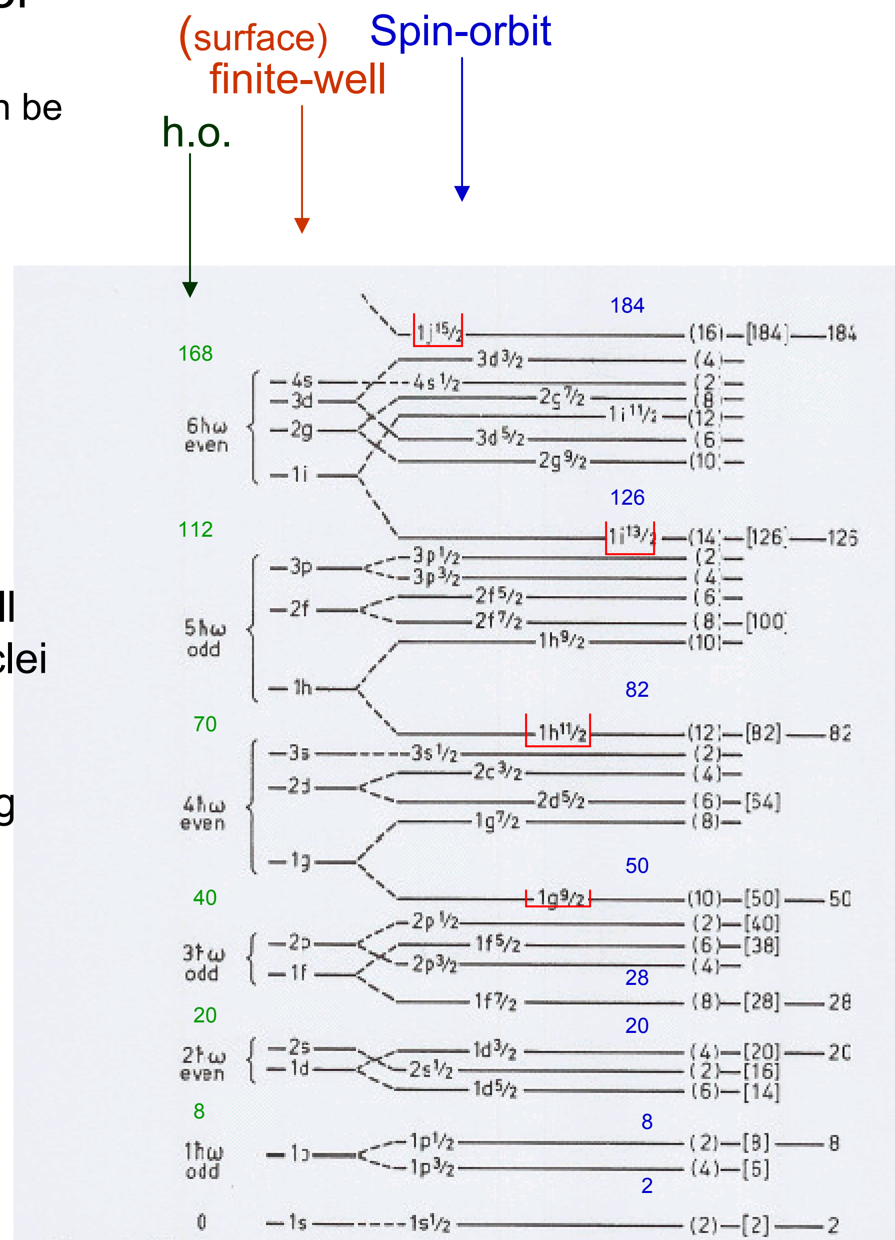

Figure 2-23 Sequence of one-particle orbits. The figure is taken from M. G. M

Phenomenological finite-well potential :

Woods-Saxon potential - an approximation to Hartree-Fock (HF) potential

$$V(r) = V_{WS}\, f(r) \qquad \text{where} \qquad f(r) = \frac{1}{1+\exp\left(\frac{r-R}{a}\right)}$$

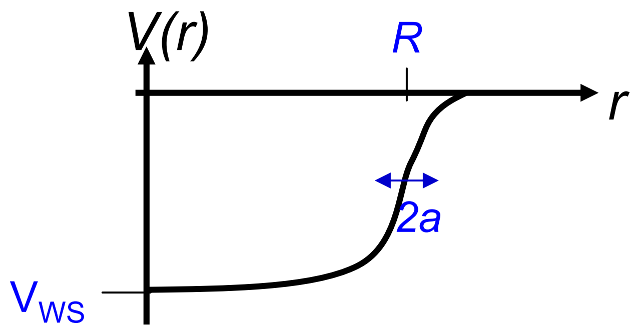

a : diffuseness

R : radius $\qquad R = r_0\, A^{1/3}$

A : mass number

standard values of parameters

$r_0 \approx 1.27$ fm $\qquad a \approx 0.67$ fm

$$V_{WS} = \left(-51 \pm 33\frac{N-Z}{A}\right) \text{ MeV}$$ for

+ for neutrons
– for protons

Woods-Saxon potential vs. harmonic-oscillator potential

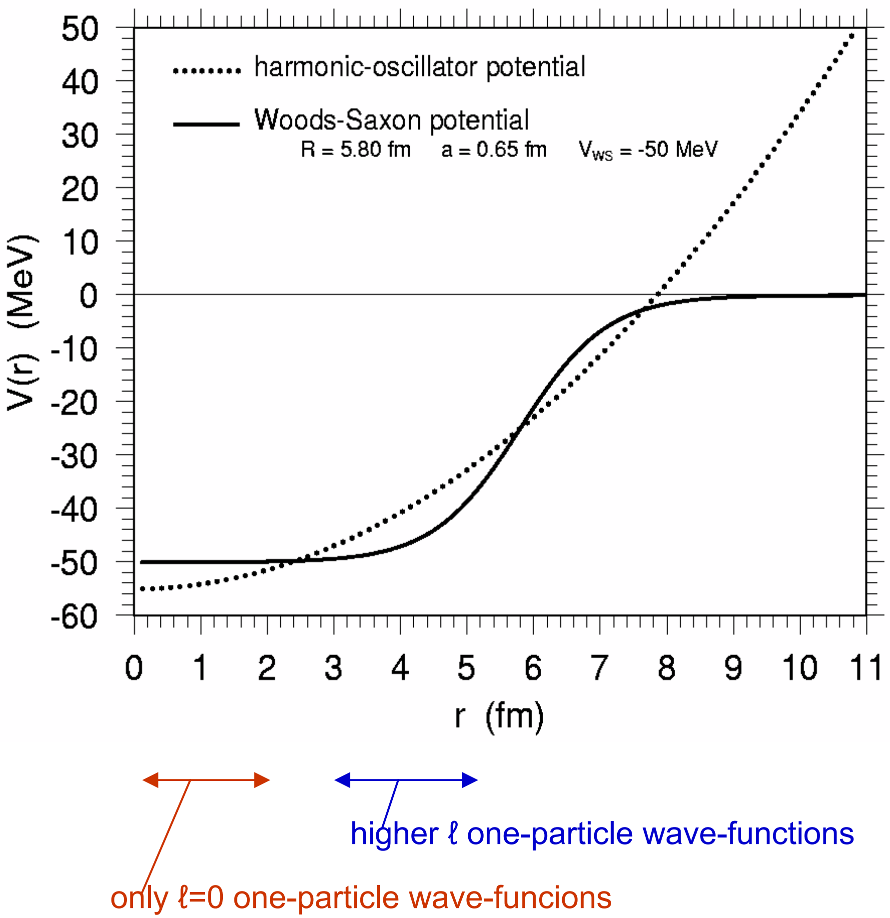

In the above figure the parameters are chosen so that the root-mean-square radius for the two potentials, are approximately equal.

Harmonic-oscillator potential cannot be used for weakly-bound or unbound (or resonant) levels.

For well-bound levels;

Corrections to harmonic-oscillator potential are;

a) repulsive effect for short and large distances

→ push up small ℓ orbits

b) attractive effect for intermediate distances

→ push down large ℓ orbits

Schrödinger equation for one-particle motion with spherical finite potentials

$$H = -\frac{\hbar^2}{2m}\left(\frac{\partial^2}{\partial x^2} + \frac{\partial^2}{\partial y^2} + \frac{\partial^2}{\partial z^2}\right) + V(r) + V_{\ell s}(r)$$

$(x, y, z) \longrightarrow (r, \theta, \varphi)$

$$H\Psi = \varepsilon\Psi \qquad \Psi = \frac{1}{r} R_{n\ell j}(r) X_{\ell j m_j}(\hat{r})$$

where

$$X_{\ell j m_j}(\hat{r}) = \sum_{m_\ell, m_s} C(\ell, \frac{1}{2}, j; m_\ell, m_s, m_j) Y_{\ell m_\ell}(\theta, \phi) \chi_{1/2, m_s}$$

$$(\vec{\ell})^2 Y_{\ell m}(\theta, \phi) = \hbar^2 \ell(\ell+1) Y_{\ell m}(\theta, \phi)$$

The Shrödinger equation for radial wave-functions is written as

$$\left\{\frac{d^2}{dr^2} - \frac{\ell(\ell+1)}{r^2} + \frac{2m}{\hbar^2}\left(\varepsilon_{n\ell j} - V(r) - V_{\ell s}(r)\right)\right\} R_{n\ell j}(r) = 0 \qquad (\$)$$

For example, for neutrons eq.($) should be solved with the boundary conditions;

at $r = 0$ $\qquad R_\ell(r) = 0$

at $r \rightarrow$ large (where $V(r) = 0$)

for $\varepsilon_\ell < 0$ $\qquad R_\ell(r) \propto \alpha r h_\ell(\alpha r)$ $\qquad$ where $\alpha^2 = -\frac{2m}{\hbar^2}\varepsilon_\ell$ $\qquad$ and $h_\ell(-iz) \equiv j_\ell(z) + i n_\ell(z)$

for $\varepsilon_\ell > 0$ $\qquad R_\ell(r) \propto \cos(\delta_\ell) kr j_\ell(kr) - \sin(\delta_\ell) kr n_\ell(kr)$ $\qquad$ where $k^2 = \frac{2m}{\hbar^2}\varepsilon_\ell$

δ_ℓ : phase shift

h_ℓ	: spherical Hankel function
j_ℓ	: spherical Bessel function
n_ℓ	: spherical Neumann function

One-body spin-orbit potential in phenomenological potentials : surface effect !

In the central part of nuclei the density, $\rho(r)$ = const.
Then, the only direction, which nucleons can feel is the momentum, $\vec{p}$

From the two vectors, $\vec{p}$ and the spin $\vec{s}$, of nucleons one cannot make

P-inv (i.e. reflection-invariant) and *T*-inv (i.e. time-reversal invariant)

quantity linear in the momentum. For example,

$(\vec{p}\cdot\vec{s})$ ~~*P*-inv~~

$(\vec{p}\times\vec{s})\cdot\vec{s}$ ~~*T*-inv~~

At the nuclear surface $\vec{\nabla}\rho(r)\neq 0$ i.e. $\vec{\nabla}\rho(r)=\left(\frac{\partial\rho}{\partial r},0,0\right)$ in polar coordinate (r,θ,φ)

$\vec{r}=(r,0,0)$

$\vec{r}\times\vec{p}=(0,-rp_{\phi},rp_{\theta})$

Then, $(\vec{p}\times\vec{s})\cdot\vec{\nabla}\rho(r)$: *P*-inv & *T*-inv !

$$=(p_{\theta}s_{\phi}-p_{\phi}s_{\theta})\frac{\partial\rho}{\partial r} = \frac{1}{r}\left((\vec{r}\times\vec{p})\cdot\vec{s}\right)\frac{\partial\rho}{\partial r}$$

$$=(\vec{\ell}\cdot\vec{s})\frac{1}{r}\frac{\partial\rho}{\partial r}$$

In practice, one often uses the form

$$V_{\ell s}(r)=\lambda(\vec{\ell}\cdot\vec{s})\frac{1}{r}\frac{\partial V_c(r)}{\partial r}$$

where λ=const. and $V_c(r)$ is one-body central potential such as the Woods-Saxon potential

In the presence of spin-orbit potential $V_{\ell s}(r)$ $(\propto (\vec{\ell}\cdot\vec{s}))$,
the total angular momentum of nucleons

$$\vec{j} = \vec{\ell} + \vec{s} \qquad j = \ell \pm \frac{1}{2}$$

becomes a good quantum-number.

$$\left[(\vec{\ell}\cdot\vec{s}), \ell_z\right] \neq 0$$

$$\left[(\vec{\ell}\cdot\vec{s}), s_z\right] \neq 0$$

$$\left[(\vec{\ell}\cdot\vec{s}), \ell_z + s_z\right] = 0$$

$$H = -\frac{\hbar^2}{2m}\Delta + V(r)$$

→ quantum number of one-particle motion (ℓ , s , m_ℓ , m_s)

$$H = -\frac{\hbar^2}{2m}\Delta + V(r) + V_{\ell s}(r)$$

→ quantum number of one-particle motion (ℓ , s , j , m_j)

$$(\vec{\ell}\cdot\vec{s}) = \frac{1}{2}\left\{\vec{j}^2 - \vec{\ell}^2 - \vec{s}^2\right\} = \frac{1}{2}\left\{ j(j+1) - \ell(\ell+1) - \frac{1}{2}(\frac{1}{2}+1)\right\} = \begin{cases} -\ell-1 & \text{for } j = \ell - 1/2 \\ \ell & \text{for } j = \ell + 1/2 \end{cases}$$

$$H\Psi = \varepsilon\Psi$$

$$\Psi = \frac{1}{r}R_{\ell j}(r)X_{\ell j m_j}$$

where $X_{\ell j m_j} \equiv \sum_{m_\ell, m_s} C(\ell, \frac{1}{2}, j; m_\ell, m_s, m_j) Y_{\ell m_\ell}(\theta,\phi)\chi_{1/2, m_s}$

The radial part of the Schrödinger equation becomes

$$\left\{\frac{d^2}{dr^2} - \frac{\ell(\ell+1)}{r^2} + \frac{2m}{\hbar^2}\left(\varepsilon_{\ell j} - V(r) - V_{\ell s}(r)\right)\right\} R_{\ell j}(r) = 0$$

Centrifugal potential + Woods-Saxon potential —— dependence on ℓ

$$-\frac{\hbar^2}{2m}\left(\frac{\partial^2}{\partial x^2}+\frac{\partial^2}{\partial y^2}+\frac{\partial^2}{\partial z^2}\right)+V(r)$$

$$=-\frac{\hbar^2}{2m}\left(\frac{1}{r}\frac{\partial^2}{\partial r^2}r+\frac{1}{r^2}\left(\frac{\partial^2}{\partial \theta^2}+\cot\theta\frac{\partial}{\partial\theta}+\frac{1}{\sin^2\theta}\frac{\partial^2}{\partial\phi^2}\right)\right)+V(r)$$

$$= -\frac{\hbar^2}{2m}\left(\frac{1}{r}\frac{\partial^2}{\partial r^2}r-\underline{\frac{1}{r^2}\frac{(\vec{\ell})^2}{\hbar^2}}\right)+V(r)$$

centrifugal potential

$\ell = 0$

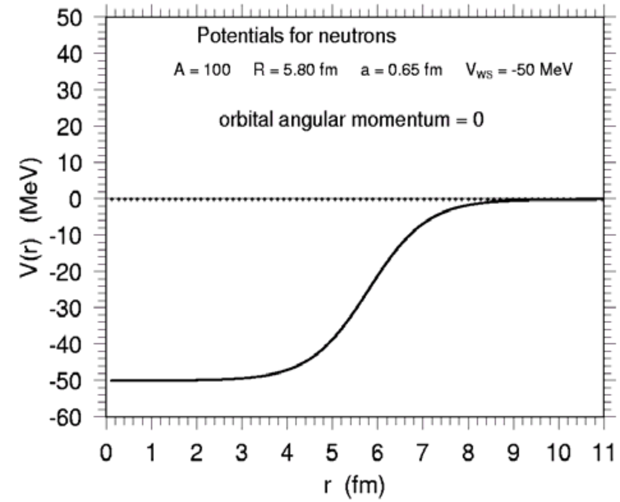

$\ell = 2$

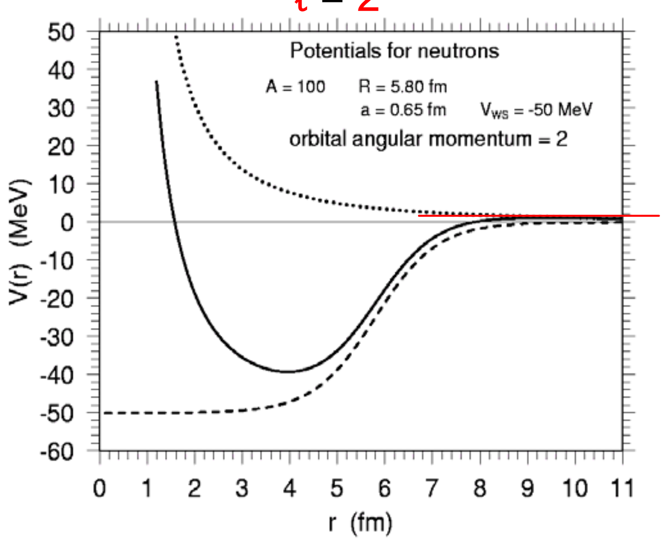

$\ell = 4$

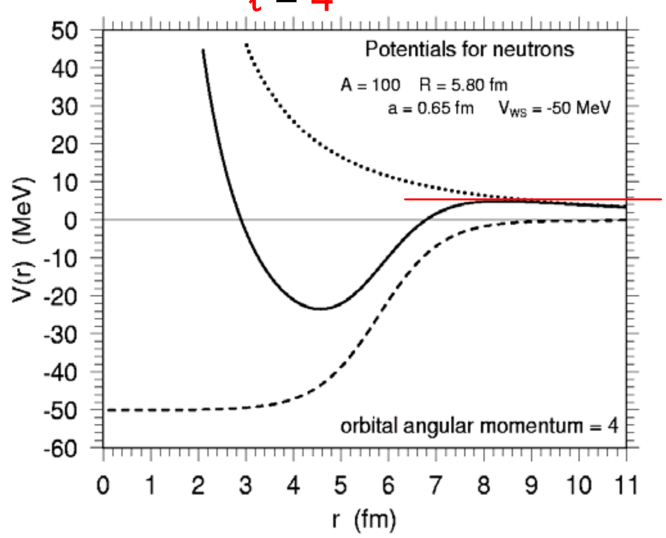

Height of centrifugal barrier $\propto \dfrac{\ell(\ell+1)}{R_h^{\,2}}$ where $R_h > r_0 A^{1/3}$

The height : $\begin{cases} \text{higher for smaller nuclei} \\ \text{higher for larger } \ell \text{ orbits} \end{cases}$

ex. For the Woods-Saxon potential with R=5.80 fm, a=0.65 fm, r_0=1.25 and V_{WS} = – 50 MeV ;

ℓ	height of centrifugal barrier
0	0 MeV
1	≈ 0.4
2	≈ 1.3
3	≈ 2.8
4	≈ 5.1
5	≈ 8.2

Height of centrifugal barrier ;

1) well-bound particles are insensitive.

2) affects eigenenergies and wave-functions of weakly-bound neutrons, especially with small ℓ

3) affects the presence (or absence) of one-particle resonance, resonant energies and widths.

Neutron radial wave-functions

$$\Psi_{n\ell jm}(\vec{r}) = \frac{1}{r}\underline{R_{n\ell j}(r)}X_{\ell jm}(\hat{r})$$

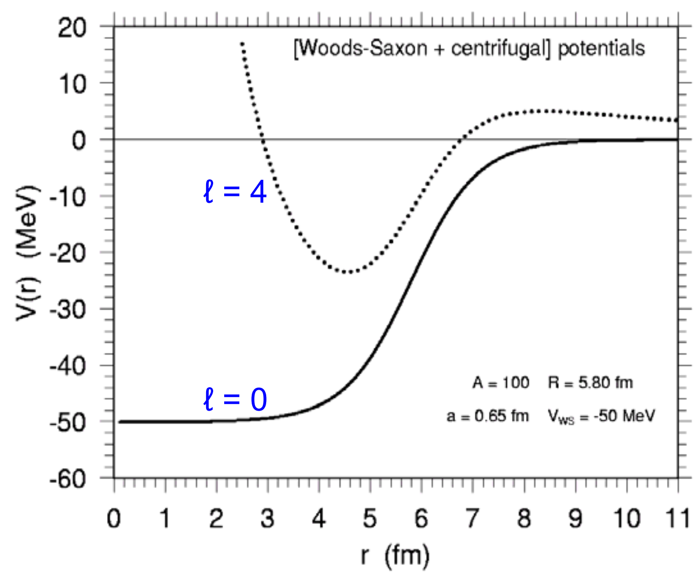

ε = – 8 MeV

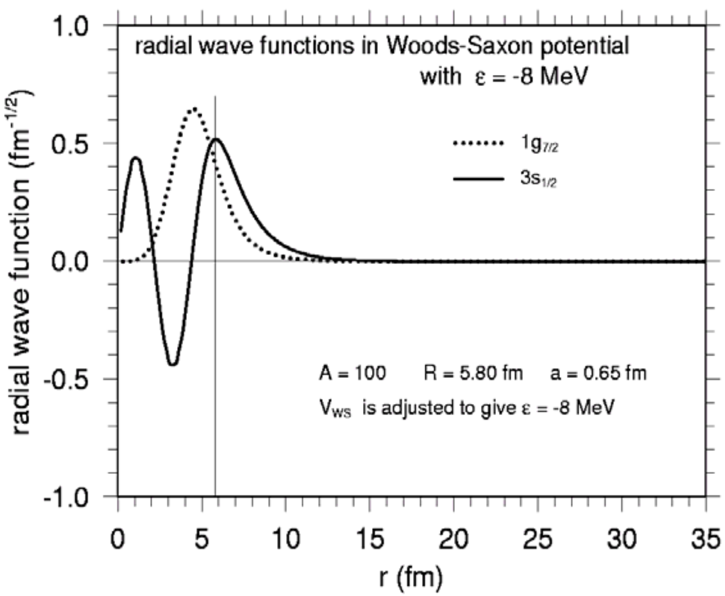

ε = – 200 keV

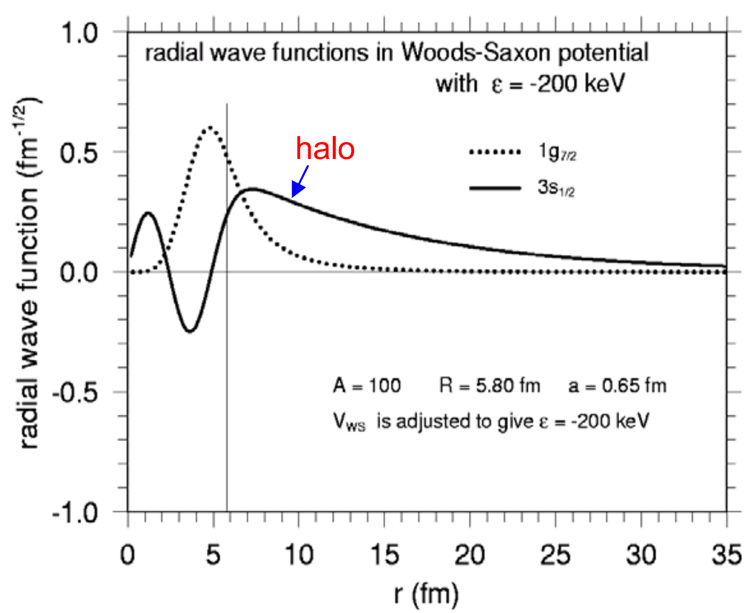

For a finite square-well potential

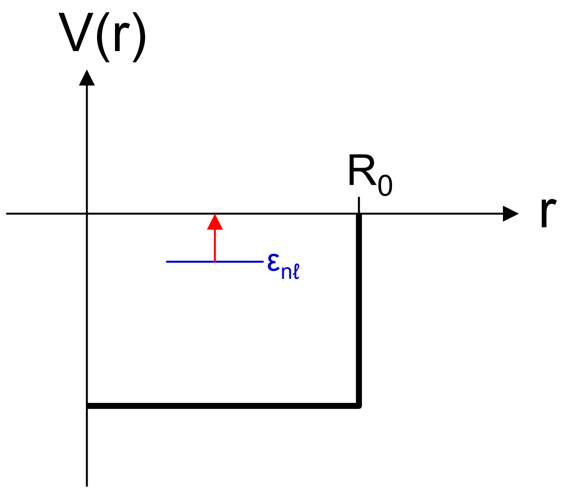

The probability for one neutron to stay inside the potential, when the eigenvalue $\varepsilon_{n\ell}$ (< 0) → 0

ℓ	0	1	2	3
$\int_0^{R_0} \|R_{n\ell}(r)\|^2 \, dr$	0	1/3	3/5	5/7

Root-mean-square radius, r_{rms}, of one neutron ; $r_{rms} \equiv \sqrt{\langle r^2 \rangle}$

In the limit of $\varepsilon_{n\ell}$ (<0) → 0

$$r_{rms} \propto (-\varepsilon_{n\ell})^{-1/2} \rightarrow \infty \quad \text{for } \ell = 0$$

$$(-\varepsilon_{n\ell})^{-1/4} \rightarrow \infty \quad \text{for } \ell = 1$$

finite value for $\ell \geq 2$

Unique behavior of low-ℓ orbits, as $E_{n\ell j}$ (<0) → 0

Energies of neutron orbits in Woods-Saxon potentials as a function of potential radius

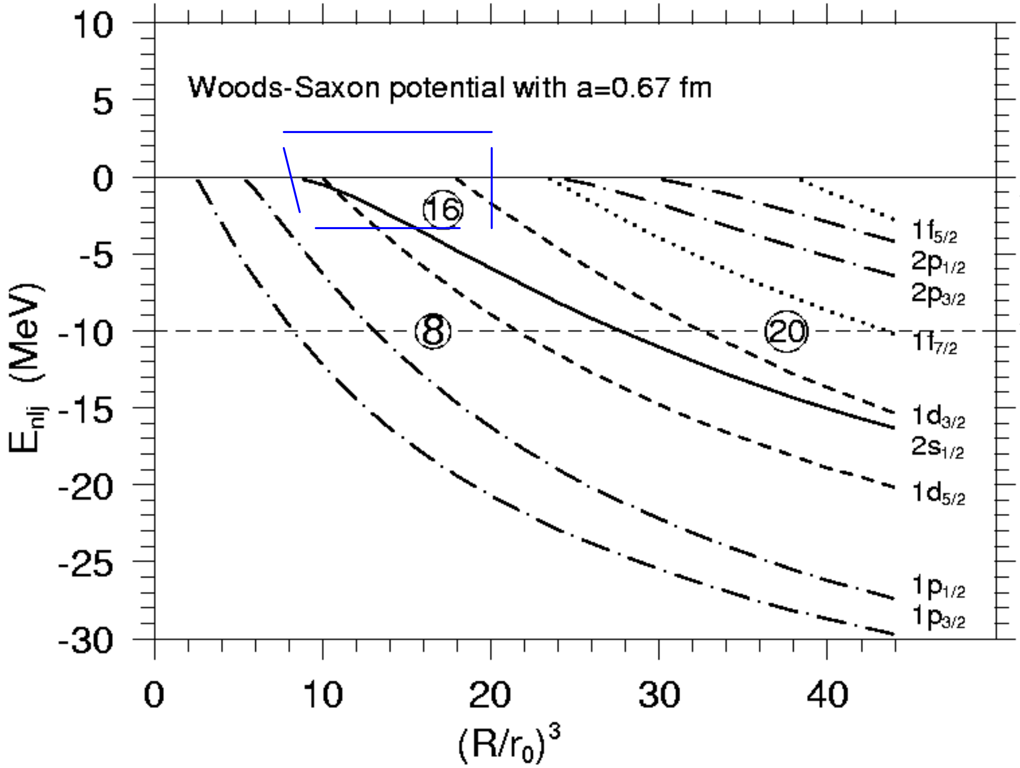

Fermi level of neutron drip line nuclei

Fermi level of stable nuclei

R = radius, r_0 = 1.27 fm,

V_{WS} = – 51 MeV

Strength of the potential

For stable nuclei

$(R/r_0)^3 \rightarrow$ A : mass number

Neutron one-particle resonant and bound levels in spherical Woods-Saxon potentials

Unique behavior of $\ell=0$ orbits, both for $\varepsilon_{n\ell j}<0$ and $\varepsilon_{n\ell j}>0$

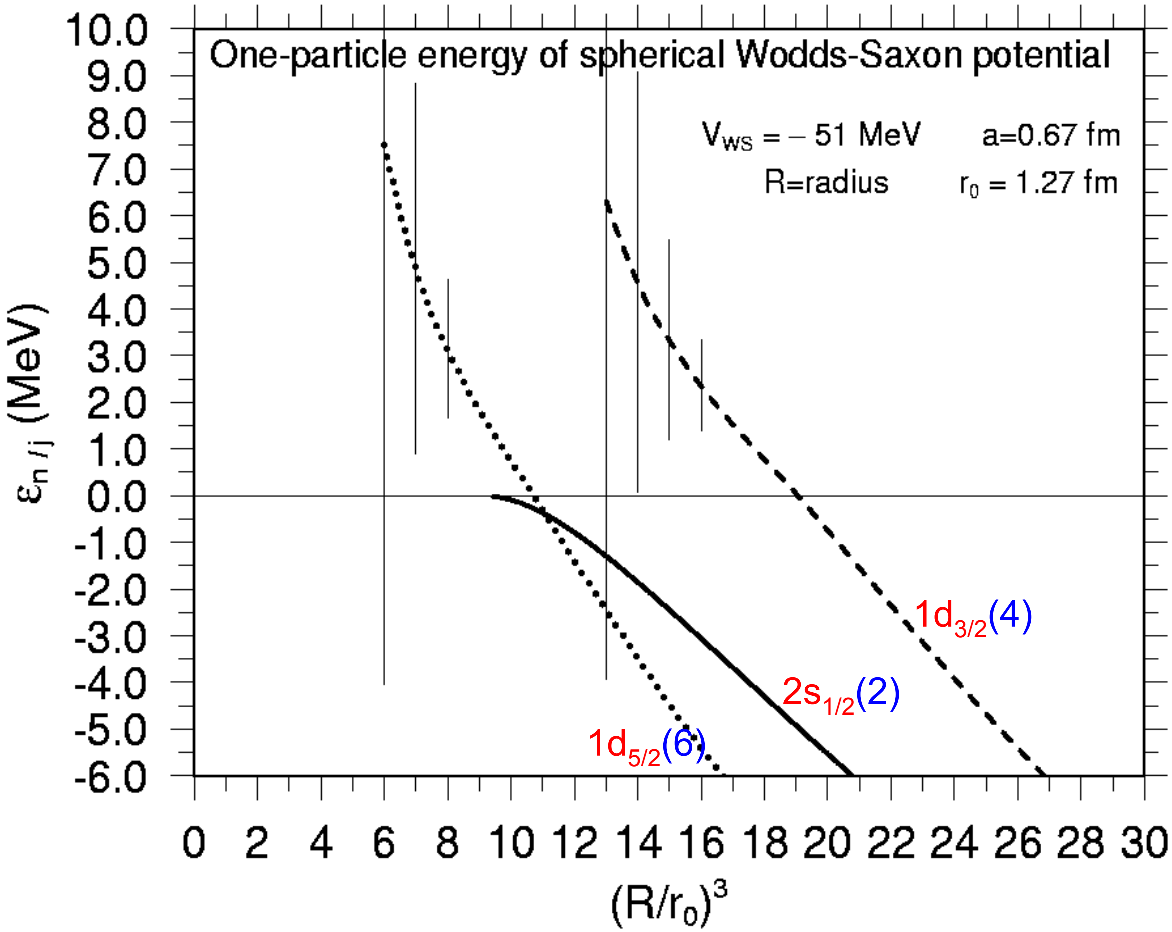

Strength of the potential

One-particle resonant levels with width

$$R_{\ell j}(r) \propto \sin\left(kr + \delta_{\ell j} - \ell\frac{\pi}{2}\right)$$

for $r \to \infty$ and $kr \equiv r\sqrt{\frac{2m\varepsilon}{\hbar^2}}$

width $\Gamma \equiv \dfrac{2}{\left.\dfrac{d\delta}{d\varepsilon}\right|_{\varepsilon=\varepsilon^{res}}}$

δ (phase shift)

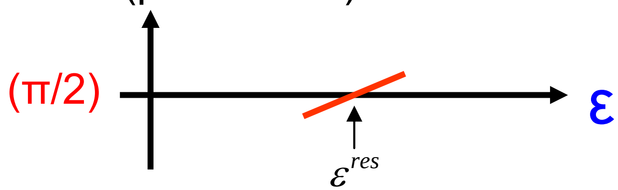

One-particle resonant level in spherical finite potentials (~~Coulomb potential~~)

For $\varepsilon_\ell > 0$ and $r \longrightarrow$ large

$$R_\ell(r) \propto \cos(\delta_\ell) kr j_\ell(kr) - \sin(\delta_\ell) kr n_\ell(kr) \qquad \text{where} \qquad k^2 \equiv \frac{2m}{\hbar^2}\varepsilon_\ell$$

δ_ℓ : phase shift

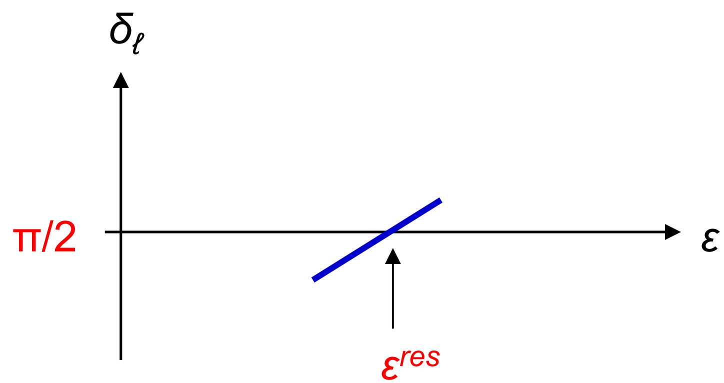

The width of the resonance;

$$\Gamma \equiv \frac{2}{\left.\frac{d\delta}{d\varepsilon}\right|_{\varepsilon=\varepsilon^{res}}}$$

The resonance energy ε^{res} is defined so that the phase shift δ_ℓ increases with energy ε as it goes through $\pi/2$ (modulo π).

For example, see ; R.G.Newton, *SCATTERING THEORY OF WAVES AND PARTICLES,* McGraw-Hill, 1966.

At ε^{res} ; (1) a sharp peak in the scattering cross section;
(2) a significant time delay in the emergence of scattered particles;
(3) the incoming wave (i.e. particles) can strongly penetrate into the system;
(4) ………..

Resonance $\leftrightarrow$ time delay $\leftrightarrow$ $\left.\frac{d\delta_\ell}{dk}\right|_{k=k_0} > 0$

scattering amplitude $f(k,\cos\theta) = k^{-1}\sum_{\ell=0}^{\infty}(2\ell+1)e^{i\delta_\ell}\sin\delta_\ell P_\ell(\cos\theta)$

For r→ ∞ , a wave packet in a scattering is written as

$$\int d\vec{k}\,\phi(\vec{k})\exp\left[i(\vec{k}\cdot\vec{r}-Et)\right]+\int d\vec{k}\,\phi(\vec{k})r^{-1}\exp\left[i(kr-Et)\right]f(k,\cos\theta) \qquad (\$)$$

where $\phi(\vec{k})$: sharply peaked around $\vec{k} = \vec{k}_0$

Assume that at $k=k_0$ a sharp peak only in a given ℓ channel.

For very large t (= time), the 2nd term in ($) contributes only at the distance

$$r \cong \frac{k_0}{2m}t - \left.\frac{d\delta_\ell}{dk}\right|_{k=k_0}$$

∵) for $k \approx k_0$ $\delta_\ell(k) \approx \delta_\ell(k_0) + \left.\frac{d\delta_\ell}{dk}\right|_{k=k_0}(k-k_0)$

$$e^{i(kr-Et)}e^{ik\left.\frac{d\delta_\ell}{dk}\right|_{k=k_0}} = e^{ik\left(r+\left.\frac{d\delta_\ell}{dk}\right|_{k=k_0}-\frac{k}{2m}t\right)}$$

Time delay caused by the sharply changing term $e^{i\delta_\ell}$ in the f : $t_D = \frac{2m}{k_0}\left.\frac{d\delta_\ell}{dk}\right|_{k=k_0}$

$\frac{d\delta_\ell}{dk} > 0$ → time delay in the emergence of the scattered particles

$\frac{d\delta_\ell}{dk} < 0$ → time advance !

β-stable nuclei

One-particle levels which contribute to many-body correlations

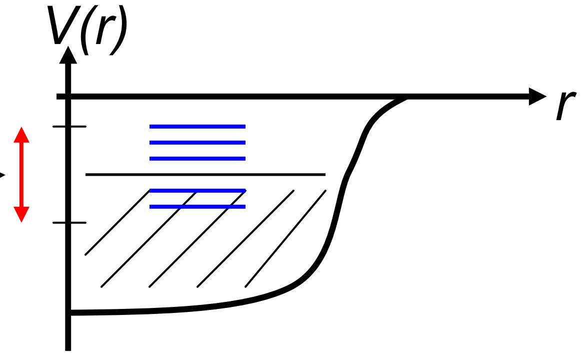

neutron drip line nuclei – role of continuum levels and weakly-bound levels

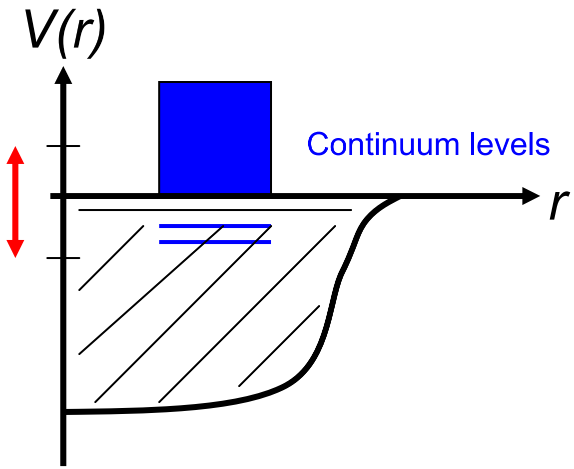

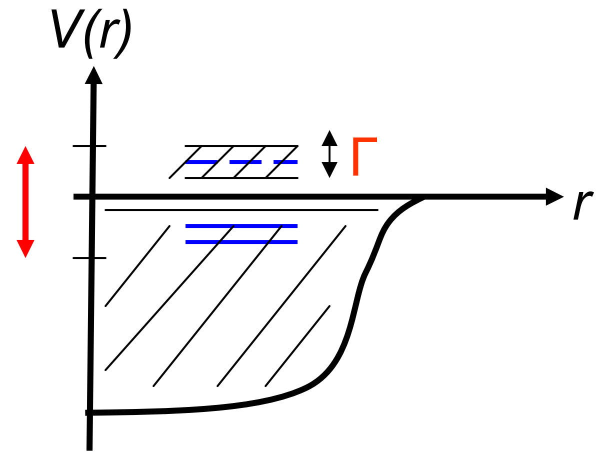

Importance of one-particle resonant levels with small width Γ in the many-body correlations.

Obs. no one-particle resonant levels for $s_{1/2}$ orbits.

A computer program to calculate one-neutron resonance (energy and width) in a spherical Woods-Saxon potential is available.

Is there anybody who wants to have it ?

Some summary of weakly-bound and positive-energy neutrons
in spherical potentials
($\beta=0$)

Unique role played by neutrons with small ℓ ; s, (p) orbits

(a) Weakly-bound small-ℓ neutrons have appreciable probability to be outside the potential;
ex. For a finite square-well potential and $\varepsilon_{n\ell j}$ (<0) → 0 , the probability inside is
0 for s neutrons
1/3 for p neutrons

Thus, those neutrons are insensitive to the strength of the potential.

→ Change of shell-structure

(b) No one-particle resonant levels for s neutrons.
Only higher-ℓ neutron orbits have one-particle resonance with small width.

→ Change of many-body correlation, such as
pair correlation and deformation
in loosely bound nuclei

2.2. Hartree-Fock (HF) approximation $\longrightarrow$ self-consistent mean-field

A mean-field approximation to the nuclear many-body problem with rotationally invariant Hamiltonian,

$$H = -\frac{\hbar^2}{2m}\sum_i \Delta_i + \sum_{i<j} v_{ij}$$

"effective" two-body interaction

phenomenology !

Popular effective interaction, v_{ij} , is so-called Skyrme interaction – many different versions exist, but

in essence, $\delta(\vec{r}_i - \vec{r}_j)$ interaction

plus density-dependent part that simulates the 3-body interaction.

The total wave function Ψ is assumed to be a form of Slater determinant consisting of one-particle wave-functions,

$\varphi_i(\vec{r}_j)$ *(i and j) = 1, 2, ….., A*

Variational principle $\delta\langle\Psi | H | \Psi\rangle = 0$

together with subsidiary conditions $\int |\varphi_i(\vec{r}_i)|^2\, d^3 r_i = 1$

leads to the HF equation.

OBS. The HF solution Ψ is not an eigen function of the Hamiltonian *H.*

ex. HF equations for 2 particles (a simple example !)

$$\Psi(1,2)=\frac{1}{\sqrt{2}}\begin{vmatrix}\varphi_1(\vec r_1) & \varphi_2(\vec r_1)\\ \varphi_1(\vec r_2) & \varphi_2(\vec r_2)\end{vmatrix}$$

$$\begin{cases} -\dfrac{\hbar^2}{2m}\Delta\varphi_1(\vec r_1)+\varphi_1(\vec r_1)\int\varphi_2^*(\vec r)v(\vec r_1,\vec r)\varphi_2(\vec r)d^3r-\varphi_2(\vec r_1)\int\varphi_2^*(\vec r)v(\vec r_1,\vec r)\varphi_1(\vec r_1)d^3r=\varepsilon_1\varphi_1(\vec r_1) \\ -\dfrac{\hbar^2}{2m}\Delta\varphi_2(\vec r_2)+\varphi_2(\vec r_2)\int\varphi_1^*(\vec r)v(\vec r_2,\vec r)\varphi_1(\vec r)d^3r-\varphi_1(\vec r_2)\int\varphi_1^*(\vec r)v(\vec r_2,\vec r)\varphi_2(\vec r_2)d^3r=\varepsilon_2\varphi_2(\vec r_2) \end{cases}$$

exchange term (absent in Hartree approximation)

Hartree potential $V_H(\vec r_1)$ and $V_H(\vec r_2)$

Find the solutions, $\varphi_1(\vec r)$ and $\varphi_2(\vec r)$, with ε_1 and ε_2 , which satisfy simultaneously the above coupled equations.

The usual procedure of solving the HF equation is;

w.f. $\varphi_1(\vec r_1)$, $\varphi_2(\vec r_2)$ → pot. $V(\vec r_1)$, $V(\vec r_2)$ → w.f. $\varphi_1(\vec r_1)$, $\varphi_2(\vec r_2)$ →

Find self-consistent solutions together with eigenvalues, ε_1 and ε_2 .

Hartree-Fock potential and one-particle energy levels

$V_N(r)$: neutron potential, $V_P(r)$: proton nuclear potential, $V_P(r)+V_C(r)$: proton total potential

A typical double-magic β-stable nucleus

$${}^{208}_{82}Pb_{126}$$

One of Skyrme interactions ;

SkM*

See : J.Bartel et al., Nucl. Phys. A386 (1982) 79.

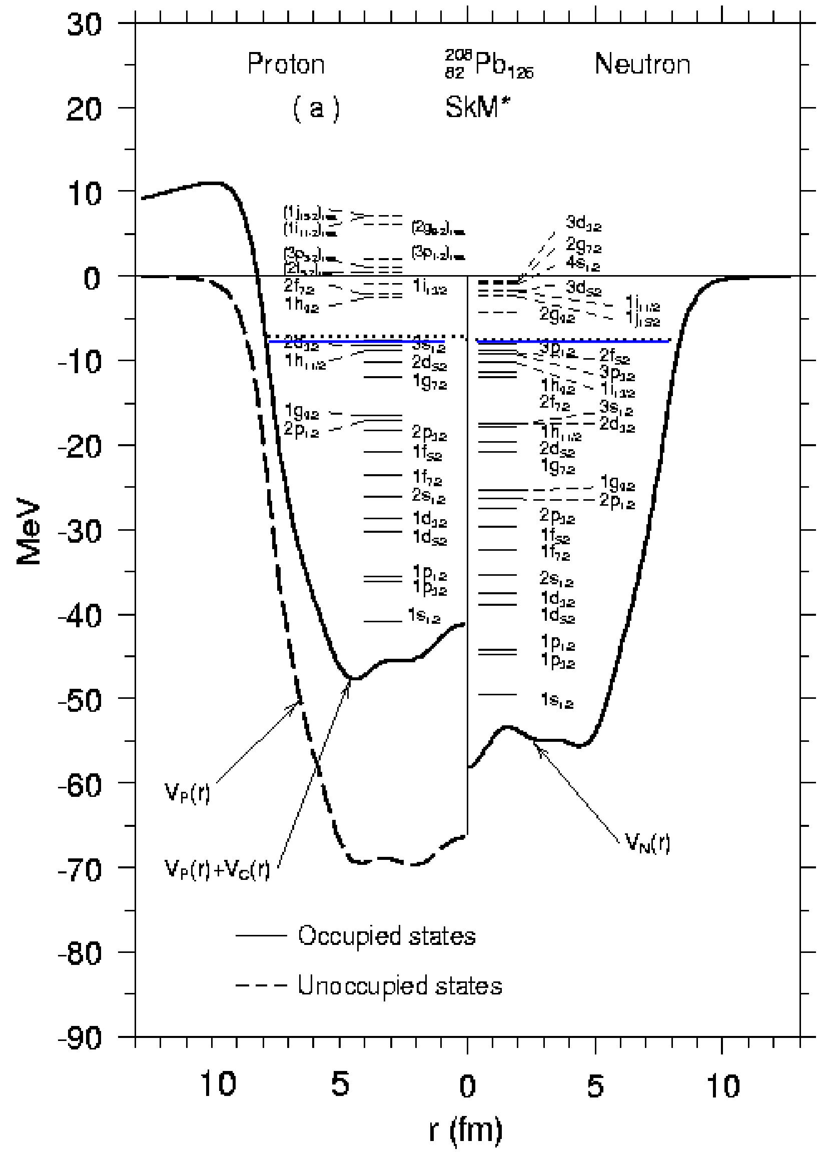

Hartree-Fock potentials and one-particle energy levels

$V_N(r)$: neutron potential, $V_P(r)$: proton nuclear potential

ex. of neutron-drip-line nuclei

ex. of proton-drip-line nuclei

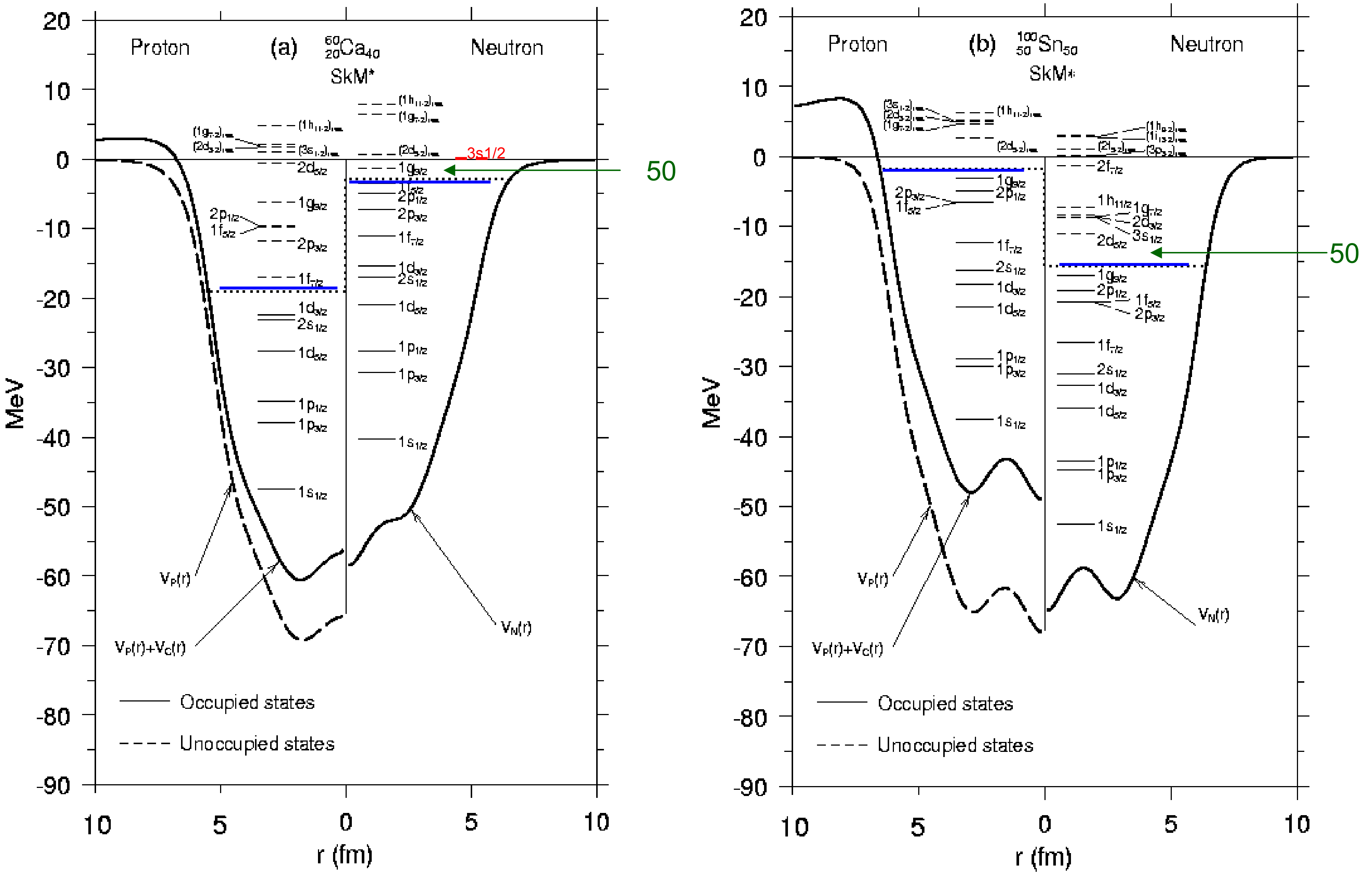

3. Observation of deformed nuclei

3.1. Rotational spectrum and its implication

Some nuclei are deformed --- axially-symmetric quadrupole (Y20) deformation

Observation :

1) rotational spectra $E(I) \approx AI(I+1)$

2) large quadrupole moment or large (E2;I→I-2) transition probability

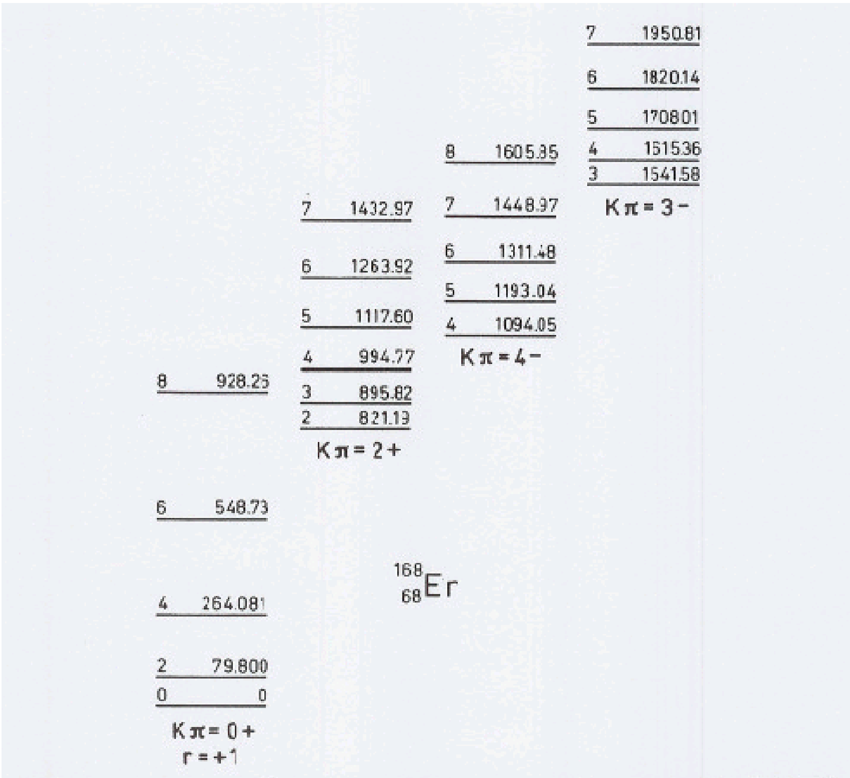

Figure 4-7 Spectrum of ^{168}Er. The data are taken from H. R. Koch, Z. Physik 192, 142

For $E(I) = AI(I+1)$,

$$\frac{E(I=4)}{E(I=2)} = 3.33$$

ex. In the ground band of ^{168}Er

$$\frac{264.081}{79.800} = 3.31$$

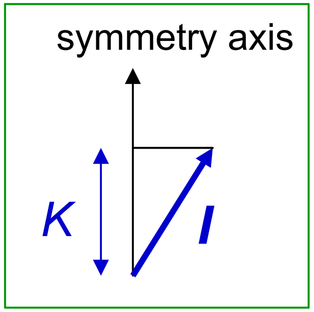

A rotational band, consisting of members with $I \geq K$.

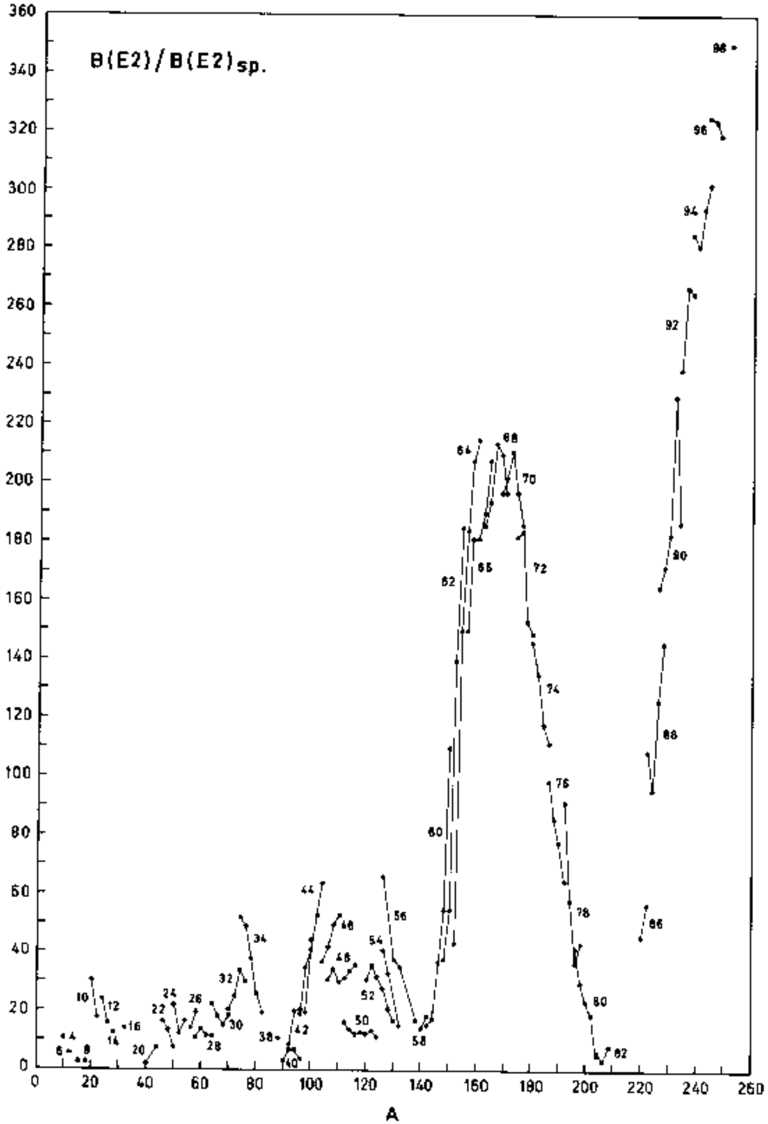

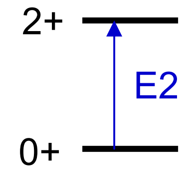

Observed E2-transition probabilities of the ground state (I=0) to the first excited 2+ state in stable even-even nuclei.

The single-particle value used as unit is

$$B_{sp}(E2) = \frac{5}{4\pi} e^2 \left(\frac{3}{5} R^2 \right)^2 = 0.30 A^{4/3} e^2 \, fm^4$$

Bohr & Mottelson, Nuclear Structure, Vol.II, 1975, Fig.4-5

WARNING : many different definitions (and notations) of Y_{20} deformation parameters

δ intrinsic quadrupole moment

$$Q_0 = \frac{4}{3}\left\langle \sum_{k=1}^{Z} r_k^2 \right\rangle \delta$$

uniformly-charged spheroidal nucleus
with a sharp surface

$$\delta = \frac{3}{2}\frac{(R_3)^2 - (R_\perp)^2}{(R_3)^2 + 2(R_\perp)^2}$$

β β_2 is defined in terms of the expansion of the density distribution in spherical harmonics.

radius $$R(\theta,\varphi) = R_0(1 + \beta_2 Y_{20}^{\ *}(\theta) + ...)$$

density $$\rho(\vec{r}) = \rho_0(r) - R_0 \frac{\partial \rho_0}{\partial r}(\beta_2 Y_{20}^{*}(\theta) + ...)$$

δ_{osc} or ε In the deformed harmonic oscillator model it is customary to use

$$\varepsilon \ = \ \delta_{osc} \equiv 3\frac{\omega_\perp - \omega_3}{2\omega_\perp + \omega_3} \approx \frac{R_3 - R_\perp}{R_{av}}$$

To leading order, $\delta \approx \beta_2 \approx \delta_{osc}$, but ....

$\delta_n \approx \delta_p$ for stable nuclei, but $\delta_n < \delta_p$ possibly for neutron-rich nuclei towards the neutron-drip-line, since $R_n > R_p$ $\because)$ $R_n\delta_n \approx R_p\delta_p$

Nuclei with deformed ground state close to the β stability line

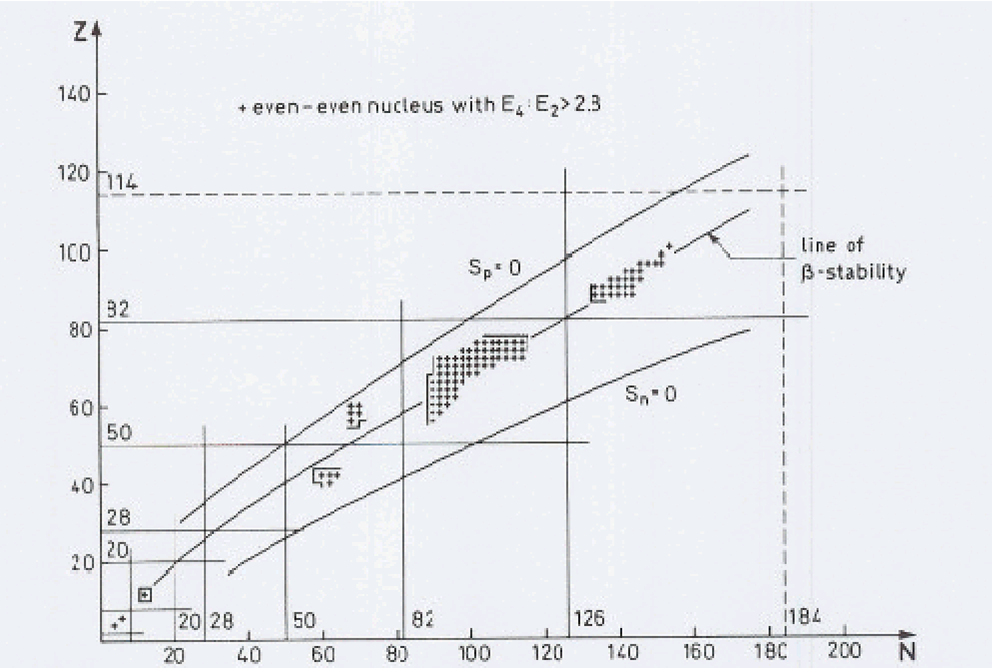

Figure 4-3 Regions of deformed nuclei. The crosses represent even-even nuclei, whose

All single or double closed-shell nuclei are spherical.

some typical examples of deformed nuclei :

$^{12}C_6$ Oblate (pancake shape)

$^{20}Ne_{10}$ Prolate (cigar shape)

rare-earth nuclei with

$$90 \le N \le 112$$

mostly prolate

Some new region of deformed ground-state nuclei away from β stability line;

1) N ≈ Z ≈ 38 ex. $^{72}_{36}Kr_{36}$ (oblate) $^{76}_{38}Sr_{38}$ (prolate ?) $^{80}_{40}Zr_{40}$ (prolate ?)

2) N ≈ 20 ex. $^{30}_{10}Ne_{20}$ $^{32}_{12}Mg_{20}$ ("island of inversion")

3) N ≈ 8 ex. $^{12}_{4}Be_{8}$ $^{11}_{4}Be_{7}$

etc.

Deformed ground state of $N \approx Z$ nuclei (proton-rich compared with stable nuclei)

Coexistence of prolate and oblate shape :

(Z=36)

Systematics of the light krypton isotopes

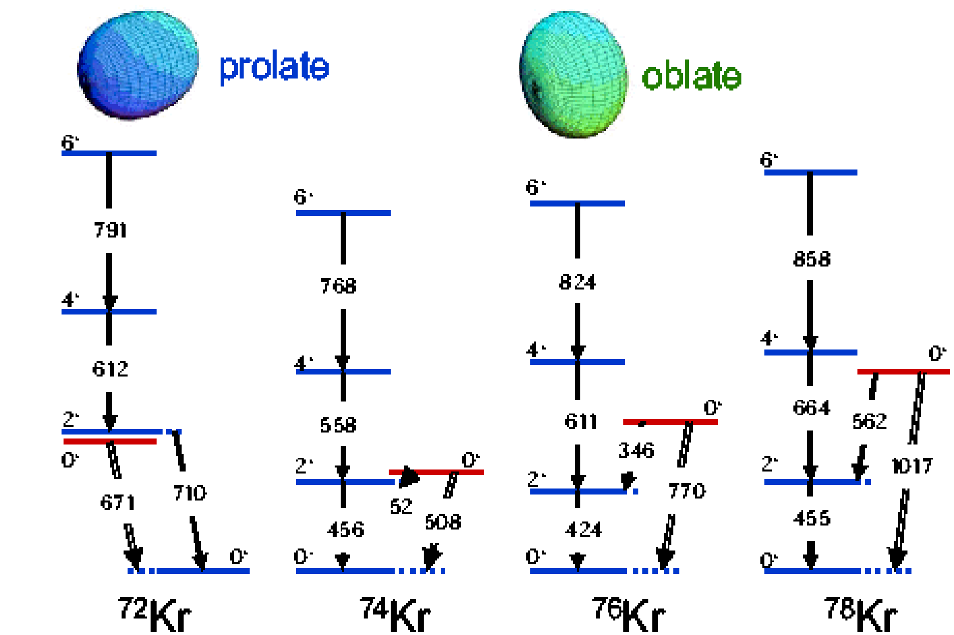

ρ²(E0) 72 · 10⁻³ 85 · 10⁻³ 79 · 10⁻³ 47 · 10⁻³

Shape of the ground state (from Coulomb excitation);

oblate prolate prolate

(A.Goergen, Gammapool workshop in Trento, 2006)

$^{76}_{38}Sr_{38}$ $^{80}_{40}Zr_{40}$

Most probably prolate

OBS. Almost all stable nuclei with N (or Z) = 40 are spherical.

Ex.

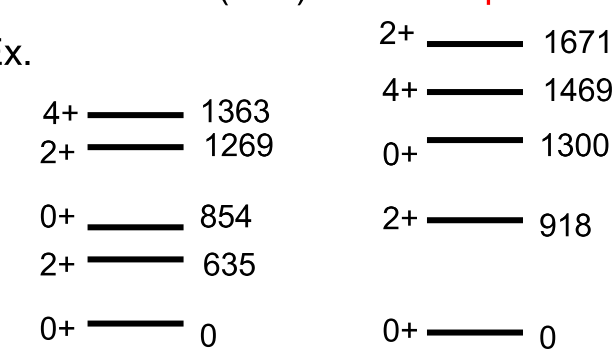

$^{74}_{34}Se_{40}$ $^{94}_{40}Zr_{54}$

S(n) = 504 keV

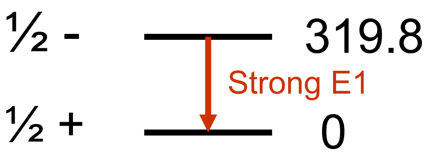

$^{11}_{4}Be_{7}$

The spin-parity of the ground state, ½+ , as well as the small energy distance between the ½ - and ½+ levels, 320 keV, is easily explained, If the nucleus is deformed !

N=8 is not a magic number !
(in this neutron-rich nucleus)

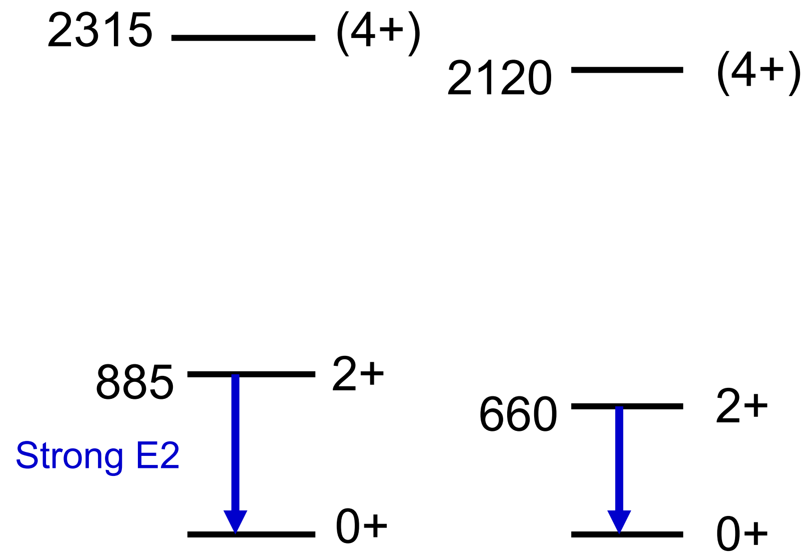

	$^{32}_{12}Mg_{20}$	$^{34}_{12}Mg_{22}$
β =	0.52	0.58
S(n) =	5.81	4.16 MeV
$\frac{E(4+)}{E(2+)}$ =	(2.62)	(3.21)

N=20 is not a magic number !
(in these neutron-rich nuclei)

Example of deformed excited states of magic nuclei

$^{40}_{20}Ca_{20}$: doubly-magic nucleus, spherical ground state

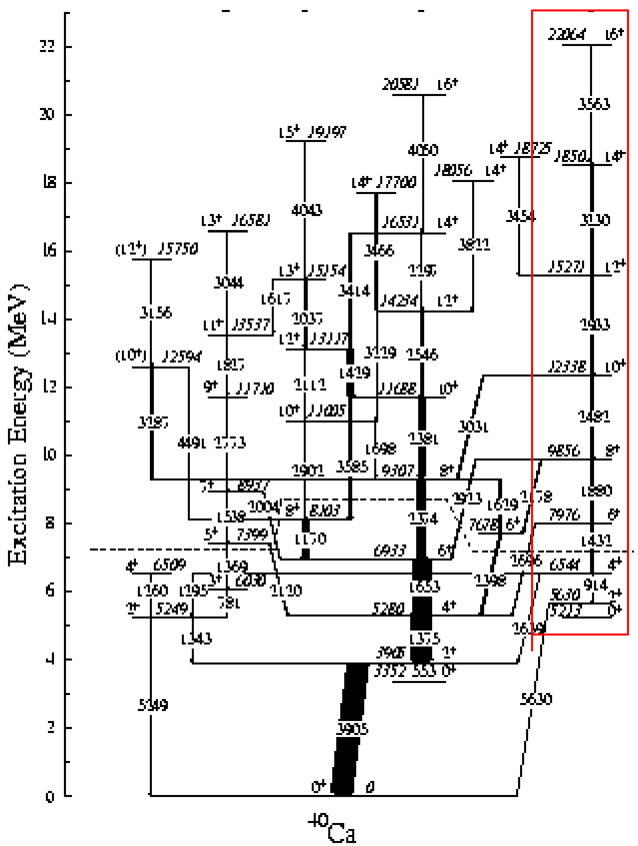

FIG. 1. Partial level scheme of ^{40}Ca; the energy labels are

strongly-deformed band

$$Q_t = 1.80 \begin{matrix} +0.39 \\ -0.29 \end{matrix} \quad \text{eb}$$

from Doppler shift measurement

$$\rightarrow \quad \beta = 0.59 \begin{matrix} +0.11 \\ -0.07 \end{matrix}$$

From E.Ideguchi et al., Phys.Rev.Lett. 87 (2001) 222501.

Implication of rotational spectra :

(1) Existence of deformation (in the body-fixed system), so as to specify an orientation of the system as a whole.

(2) Collective rotation, as a whole, and internal motion w.r.t. the body-fixed system are approximately separated in the complicated many-body system.

Classical system : An infinitesimal deformation is sufficient to establish anisotropy.

Quantum system : [zero-point fluctuation of deformation] $\ll$ [equilibrium deformation], in order to have a well-defined rotation.

Indeed,

collective rotation is the best established collective motion in nuclei.

For some nuclei Hartree-Fock (HF) calculations with rotationally-invariant Hamiltonian end up with a deformed shape !

spherical shape $\leftarrow$ HF solutions for “closed-shell” nuclei

deformed shape $\leftarrow$ HF solutions for some nuclei

$\swarrow\nearrow$ exhibit rotational spectra

$\therefore$ Deformed shape obtained from HF calculations is interpreted as the intrinsic structure (in the body-fixed system) of the nuclei.

The notion of one-particle motion in deformed nuclei can be, in practice, much more widely, in a good approximation, applicable than that in spherical nuclei.

$\because$) The major part of the long-range two-body interaction is already taken into account in the deformed mean-field.

Thus, the spectroscopy of deformed nuclei is often much simpler than that of spherical vibrating nuclei.

What can one learn from rotational spectra ?

(a) Quantum numbers of rotational spectra ↔ symmetry of deformation

ex. Parity is a good quantum number ← space reflection invariance,
K is a good quantum number ← Axially-symmetric shape ($E(I) \propto I(I+1)$) ,
where K is the projection of angular momentum along the symmetry axis.
The K=0 rotational band has only I = 0, 2,4,… ← shape is *R*- invariant,
Kramers degeneracy ← time reversal invariance,
etc.

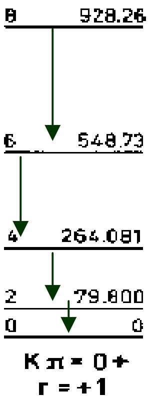

(b) rotational energy, E(I) - E(I-2)
E2 transition probability ↓
} ↔ size of deformation

R-invariant shape : in addition to axially-symmetry, the shape is further invariant w.r.t. a rotation of π about an axis perpendicular to the symmetry axis.
(If a shape is already axial symmetric, reflection invariance is equivalent to *R*-inv.)
ex. Y_{20} deformed shape is *R*-invariant, but not Y_{30} deformed shape.

Kramers degeneracy : The levels in an odd-fermion system are at least doubly degenerate.

Why are some nuclei deformed ?

Usual understanding ;

Deformation of ground states (ND, $R_\perp : R_z \approx 1 : 1.3$) ← Jahn-Teller effect

Many particles outside a closed shell in a spherical potential
→ near degeneracy in quantum spectra
→ possibility of gaining energy by breaking away from spherical symmetry using the degeneracy

Superdeformation (SD, $R_\perp : R_z \approx 1 : 2$) at high spins in rare-earth nuclei or fission isomers in actinide nuclei
← new shell structure (and new magic numbers !) at large deformation

3.2. Important deformation and quantum numbers in deformed nuclei

Axially symmetric quadrupole (Y20) deformation (plus *R*-symmetry)
- most important deformation in nuclei

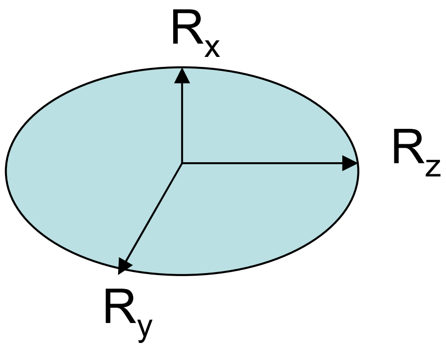

$R_\perp (= R_x = R_y) < R_z$ prolate (cigar shape)

$R_\perp (= R_x = R_y) > R_z$ oblate (pancake shape)

Axially-symmetric quadrupole-deformed harmonic-oscillator potential

$$H = T + V \quad \text{with} \quad V = \frac{M}{2}\left(\omega_z^2 z^2 + \omega_\perp^2 (x^2 + y^2)\right)$$

$$H\left|n_x, n_y, n_z\right\rangle = \varepsilon(n_\perp, n_z)\left|n_x, n_y, n_z\right\rangle \quad \text{where} \quad n_\perp = n_x + n_y$$

$$\varepsilon(n_\perp, n_z) = (n_z + \frac{1}{2})\hbar\omega_z + (n_\perp + 1)\hbar\omega_\perp = \hbar\varpi\left(N + \frac{3}{2} - \frac{\delta}{3}(3n_z - N)\right)$$

where $\varpi = \frac{1}{3}(\omega_z + 2\omega_\perp)$ and $N = n_x + n_y + n_z$

deformation parameter $\delta \equiv 3\frac{\omega_\perp - \omega_z}{2\omega_\perp + \omega_z} \approx \frac{R_z - R_\perp}{R_{av}}$

$\delta > 0 \rightarrow R_z > R_\perp$: prolate

$\delta < 0 \rightarrow R_z < R_\perp$: oblate

One-particle spectrum of Y20-deformed harmonic-oscillator potential

$$\varepsilon(N,n_z) = \hbar\varpi(N + \frac{3}{2} - \frac{\delta}{3}(3n_z - N))$$

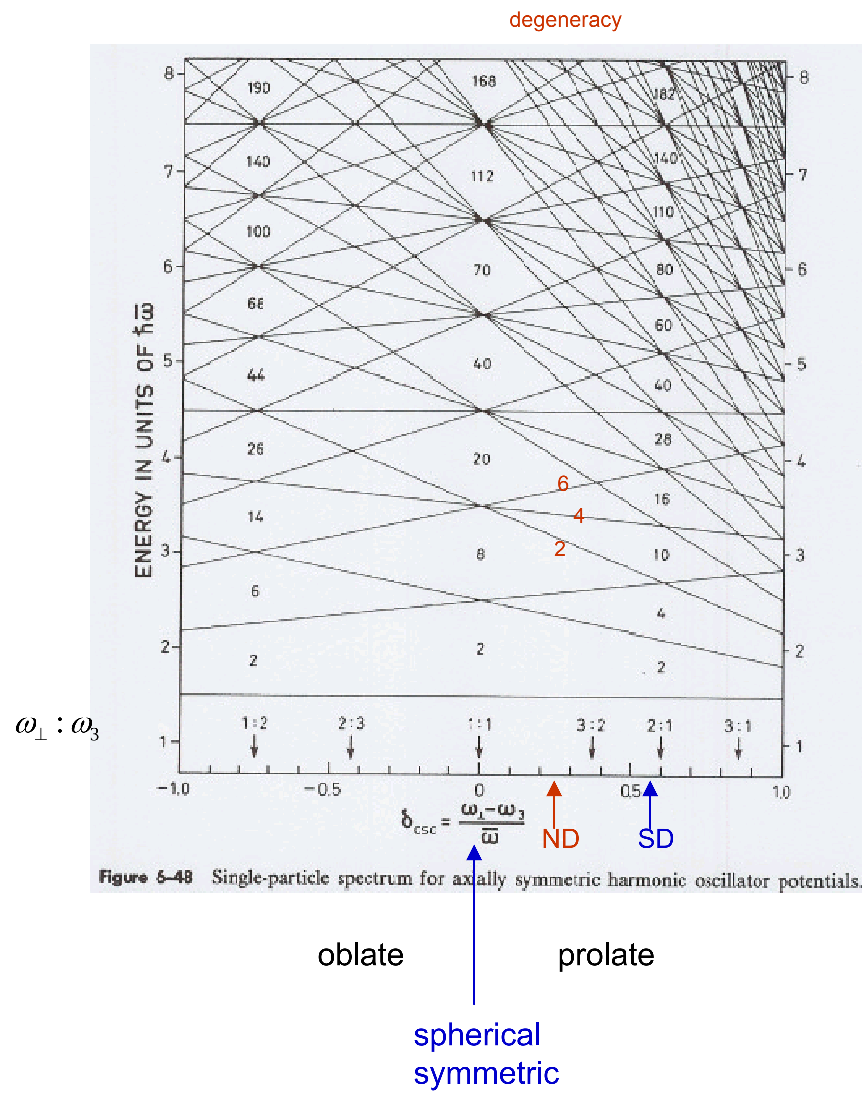

Figure 6-48 Single-particle spectrum for axially symmetric harmonic oscillator potentials.

(1) At δ = 0 : spherical,

$$\varepsilon(N) = \hbar\varpi(n_x + n_y + n_z + \frac{3}{2}) = \hbar\varpi(N + \frac{3}{2})$$

degeneracy (*N*+1)(*N*+2)

(2) At δ ≠ 0

ε(N) splits into *(N+1) levels,* $\varepsilon(N, n_z)$

$\because$) n_z = 0, 1, 2, ……., *N*

The level with $\varepsilon(N, n_z)$ has degeneracy

$2(n_\perp + 1)$

Spin ↑↓

$\because$) $N - n_z = n_\perp = n_x + n_y$ and

n_y = 0, 1, ……., $n_\perp$

(3) Note "closed shell" appears, when $\omega_\perp : \omega_z$ is a small integer ratio. ⟶ large degeneracy

ex. $\omega_\perp = 2\omega_z \longrightarrow \varepsilon(N, n_z) = \hbar\omega_z(n_z + 2n_\perp + 2 + \frac{1}{2})$

where one can have many combinations of integer (n_z, $n_\perp$) values that give the same value of ($n_z + 2n_\perp$).

One-particle Hamiltonian with spin-orbit potential

$$H = T + V(r,\theta)$$

$$V(r,\theta) = V_0(r) + V_2(r) Y_{20}(\theta) + V_{\ell s}(r)(\vec{\ell} \cdot \vec{s}) \qquad Y_{20}(\theta) = \sqrt{\frac{5}{16\pi}}(3\cos^2\theta - 1)$$

where θ is polar angle w.r.t. the symmetry axis (= z-axis)

Quantum numbers of one-particle motion in *H*

(1) Parity $\pi = (-1)^{\ell}$ where ℓ is orbital angular momentum of one-particle.

(2) $\Omega \leftarrow \ell_z + s_z$ $\because$)

$[\, f(r)\, Y_{20}(\theta)\, ,\, \ell_z + s_z\,] = 0$ and $\left[(\vec{\ell} \cdot \vec{s}), \ell_z + s_z\right] = 0$

4. One-particle motion sufficiently bound in Y_{20} deformed potential

$$V(r,\theta) = V_0(r) + V_2(r)Y_{20}(\theta) + V_{\ell s}(r)(\vec{\ell}\cdot\vec{s})$$

4.1. Normal-parity orbits and/or large deformation

$$\langle V_2(r)Y_{20}(\theta)\rangle >> \langle V_{\ell s}(r)(\vec{\ell}\cdot\vec{s})\rangle$$

$$H_0 = T + \frac{M}{2}(\omega_z^2 z^2 + \omega_\perp^2(x^2+y^2))$$

$$H' = V_{\ell s}(r)(\vec{\ell}\cdot\vec{s})$$

$$\varepsilon(N,n_z) = (n_z + \frac{1}{2})\hbar\omega_z + (n_\perp + 1)\hbar\omega_\perp$$

has $2(n_\perp + 1)$ degeneracy. $n_\perp = n_x + n_y$

The degeneracy can be resolved by specifying $n_x = 0, 1, \ldots, n_\perp$ for a given $n_\perp$. However, since $[H_0, \ell_z] = 0$, (ℓ_z : z-component of one-particle orbital angular momentum), quantum number Λ ($\leftarrow \ell_z$) can be used to resolve the $(n_\perp + 1)$ degeneracy.

Possible values of Λ are $\Lambda = \pm n_\perp, \pm(n_\perp - 2), \ldots\ldots, \pm 1$ or 0.

The basis $[n_\perp, n_z, \Lambda]$ is useful for $H' \propto (\vec{\ell}\cdot\vec{s})$

Including spin, $\Sigma \leftarrow s_z$,

$$\langle n_\perp n_z \Lambda\Sigma | H | n_\perp n_z \Lambda\Sigma\rangle = \varepsilon(n_\perp, n_z) + \langle n_\perp n_z | V_{\ell s}(r) | n_\perp n_z\rangle \Lambda\Sigma$$

$[n_\perp n_z \Lambda\Sigma]$ or $[N\, n_z\, \Lambda\, \Omega]$: asymptotic quantum numbers

$N = n_\perp + n_z$ and $\Omega = \Lambda + \Sigma$

$[\, N\, n_z\, \Lambda\, \Omega \,]$: approximately good quantum numbers for large Y_{20} deformation

(Ω is an exact quantum-number)

Thus, in deformed nuclei it is customary to denote

observed one-particle levels, or
one-particle levels obtained from finite-well potentials, or
HF one-particle levels etc.

by $[\, N\, n_z\, \Lambda\, \Omega \,]$, in which $|N n_z \Lambda \Omega>$ is the major component of the wave functions.

Denote $\Omega > 0$ value, though $\pm\,\Omega$ doubly degenerate (Kramers degeneracy).

---

ex. For deformation $\delta = 0.3$ the proton one-particle wave-functions obtained by diagonalizing $H = T + V(r,\theta)$ with a $(\boldsymbol{\ell}\cdot\boldsymbol{s})$ potential are

$|\,[411\ 3/2]> \;=\; 0.926\,|\,411\ 3/2> + \dots \;= 0.418\,|g_{9/2}> -0.140\,|g_{7/2}> +0.864\,|d_{5/2}> +0.246\,|d_{3/2}>$
$|\,[411\ 1/2]> \;=\; 0.900\,|\,411\ 1/2> + \dots \;= -0.163\,|g_{9/2}> +0.396\,|g_{7/2}> -0.099\,|d_{5/2}> +0.848\,|d_{3/2}> +0.297\,|s_{1/2}>$
$|\,[400\ 1/2]> \;=\; 0.968\,|\,400\ 1/2> + \dots \;= 0.147\,|g_{9/2}> -0.072\,|g_{7/2}> +0.539\,|d_{5/2}> -0.160\,|d_{3/2}> +0.811\,|s_{1/2}>$

(From A.Bohr & B.R.Mottelson, Nuclear Structure, vol.II, Table 5-2.)

$$V(r,\theta) = V_0(r) + V_2(r)Y_{20}(\theta) + V_{\ell s}(r)(\vec{\ell}\cdot\vec{s})$$

4.2. high-j orbits and/or small deformation

$$\langle V_2(r)Y_{20}(\theta)\rangle << \langle V_{\ell s}(r)(\vec{\ell}\cdot\vec{s})\rangle$$

those pushed down by $(\vec{\ell}\cdot\vec{s})$ potential : ex. $g_{9/2}$, $h_{11/2}$, $i_{13/2}$, …

j (= one-particle angular momentum) is approximately a good quantum number.

$$H_0 = T + V_0 + V_{\ell s}(r)\,(\vec{\ell}\cdot\vec{s})$$

$$H' = V_2(r)\; Y_{20}(\theta)$$

For a single-j shell,

$$H_0 |\ell j> = \varepsilon_0(\ell j)\, |\ell j>$$

$$H\, |\, \ell j\Omega> = \varepsilon(\ell j\Omega)\, |\, \ell j\Omega>$$

$$\varepsilon(\ell j\Omega) = \varepsilon_0(\ell j) + <\ell j\Omega\, |\, H'\, |\, \ell j\Omega>$$

$$= \varepsilon_0(\ell j) + \frac{3\Omega^2 - j(j+1)}{4j(j+1)}\left\langle \ell j \middle| -\sqrt{\frac{5}{4\pi}}V_2(r) \middle| \ell j\right\rangle$$

|| deformation parameter

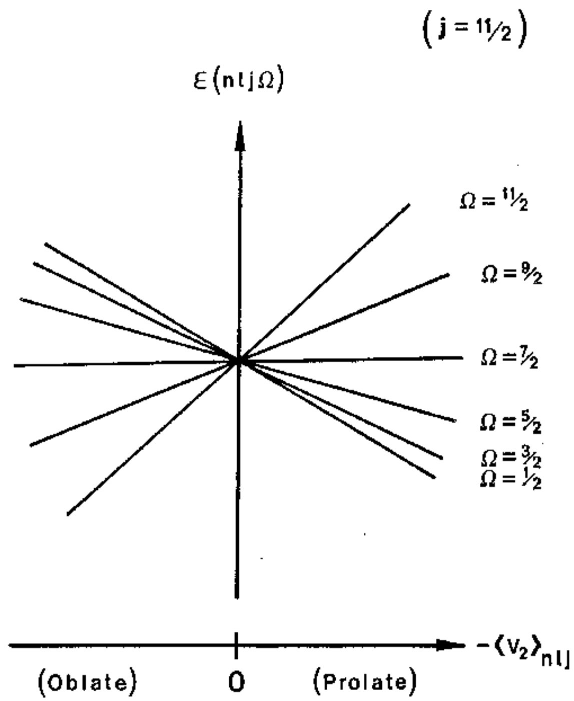

spherical : (2j+1) degeneracy ⟶ Y_{20} deformed : ± Ω degeneracy

4.3. “Nilsson diagram” — one-particle spectra as a function of deformation

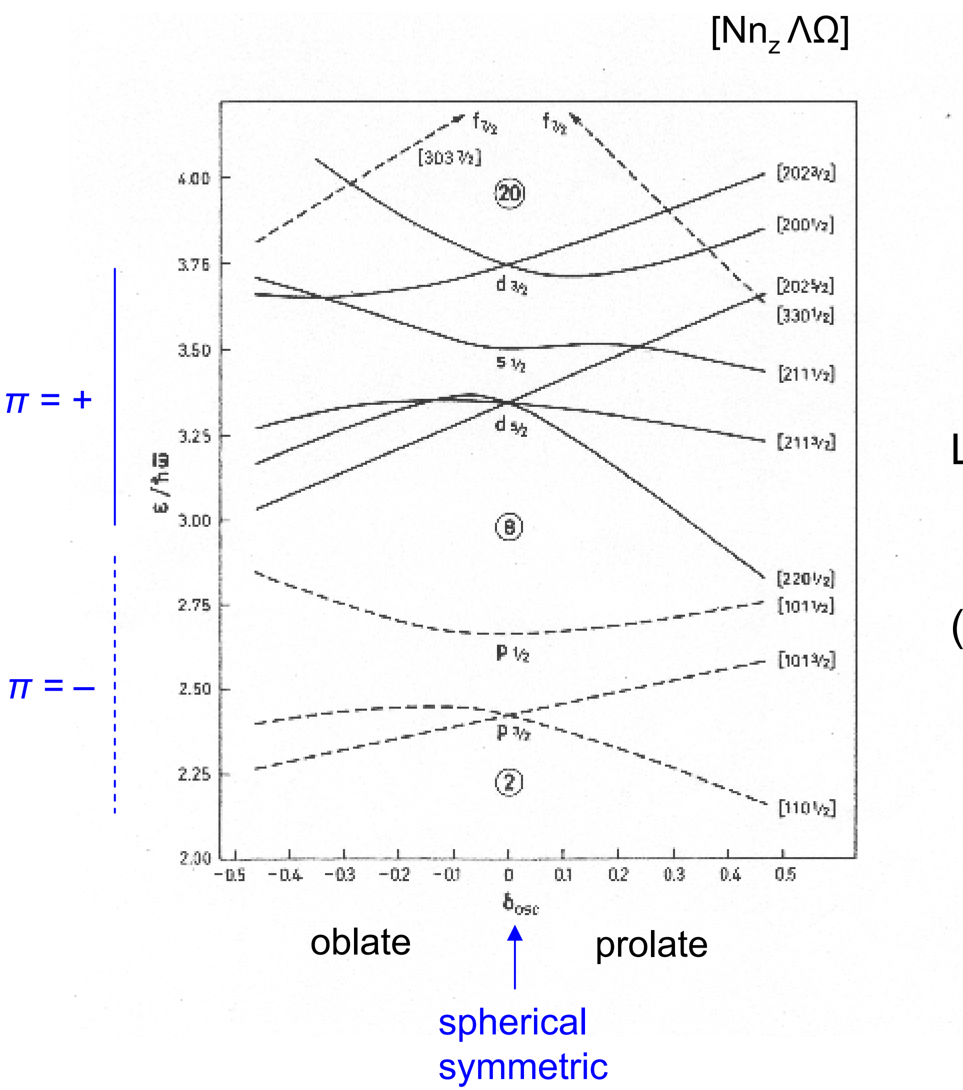

Diagonalize $H = T + V(r,\theta)$

where

$$V(r,\theta) = V_0(r) + \underline{V_2(r)Y_{20}(\theta)} + \underline{V_{\ell s}(r)(\vec{\ell}\cdot\vec{s})}$$

Levels are doubly degenerate with $\pm\Omega$.

(π, Ω) : exact quantum numbers.

Levels with a given (π, Ω) interact !

i.e. levels with the same (π, Ω) never cross !

Proton orbits in prolate potential (50 < Z < 82).

$g_{7/2}$, $d_{5/2}$, $d_{3/2}$ and $s_{1/2}$ orbits, which have $\pi = +$, do not mix with $h_{11/2}$ by Y_{20} deformation.

$h_{11/2}$ orbit
= high-j orbit
with $\pi = -$

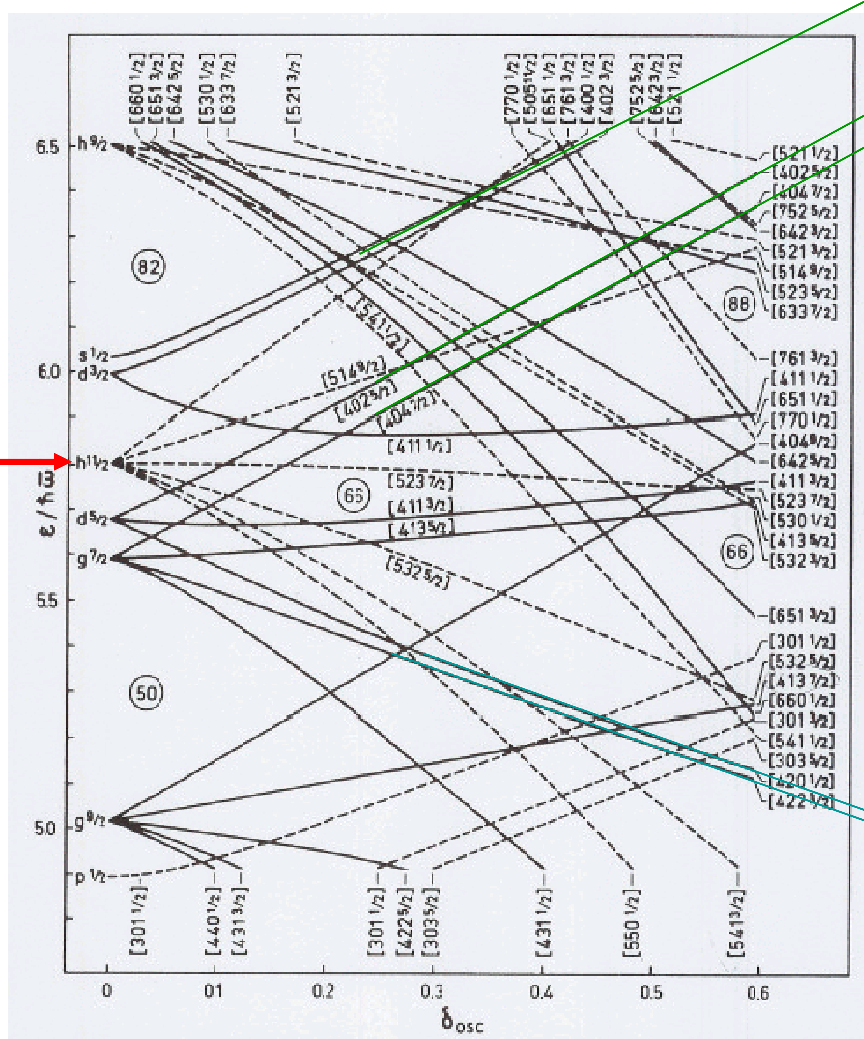

Figure 5-2 Proton orbits in prolate potential (50 < Z < 82). The spectra in this and the

[N=4, n_z =0]

[N=4, n_z =2]

Levels are doubly degenerate with $\pm\,\Omega$.

At small δ and $h_{11/2}$ orbit,

$$\varepsilon \;\propto\; \delta\,(3\Omega^2 - j(j+1)\,)$$

At large δ,

$$\varepsilon \;\propto\; -\,\delta(3n_z - N)$$

At δ > 0.3 for prolate shape quantum numbers [$Nn_z\Lambda\Omega$] work well, except for high-j orbits.

Intrinsic configuration in the body-fixed system

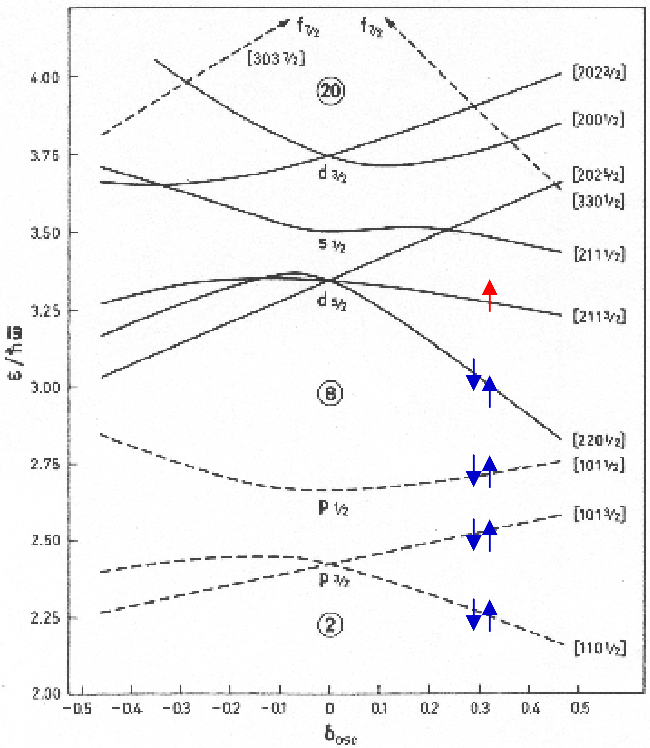

Low-lying states in deformed odd-A nuclei may well be understood in terms of the $[Nn_z \Lambda\Omega]$ orbit of the last unpaired particle.

Good approximation ;

(a) In the ground state of eve-even nuclei

$$K \equiv \sum_{i=1}^{A} \Omega_i = 0$$

Namely, $\pm\,\Omega$ levels are pair-wise occupied.

(b) In low-lying states of odd-A nuclei

$$K \equiv \sum_{i=1}^{A} \Omega_i \quad \Rightarrow \quad \Omega \text{ of the last unpaired particle.}$$

ex. The N=13 th neutron orbit is seen in low-lying excitations in $^{25}Mg_{13}$

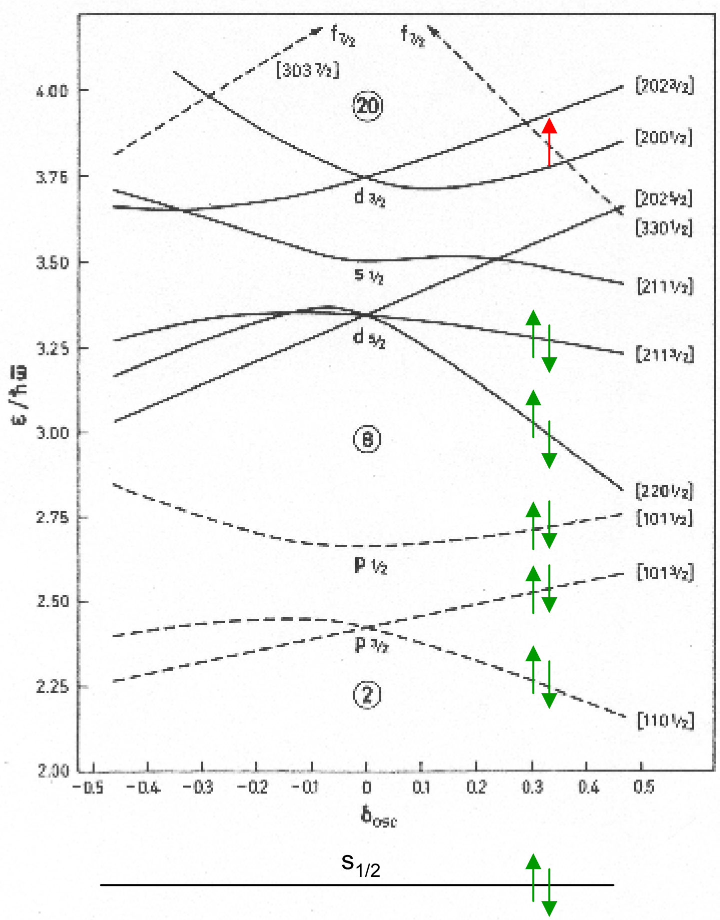

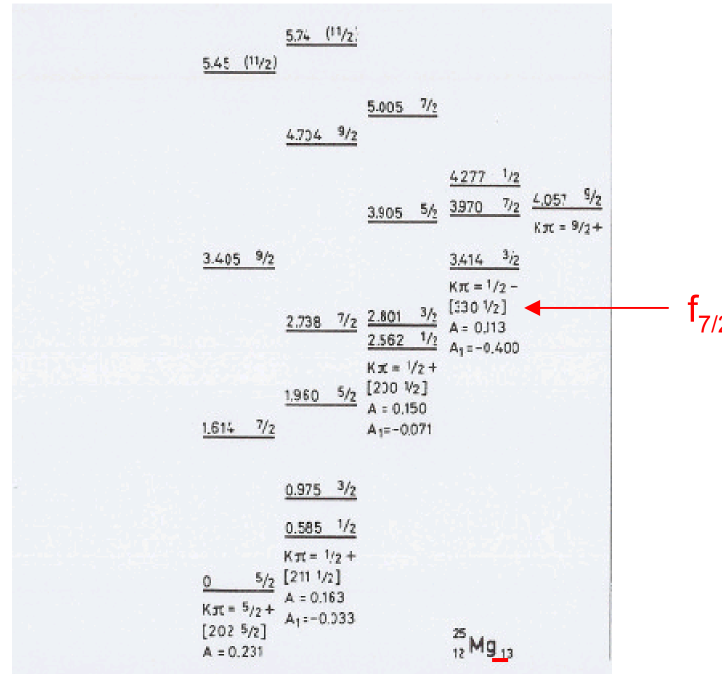

Figure 5-15 Spectra of ^{25}Mg and ^{25}Al. The recognition of rotational ba

Note (a) $I \geq K$ ($\leftarrow I_3$)

(b) the bandhead state has I=K.
Exception may occur for K=1/2 bands.

(c) some irregular rotational spectra are observed for K=1/2 bands.

1) Leading-order E2 and M1 intensity relation works pretty well

$\rightarrow$ $Q_0 \approx +50$ fm^2 $\rightarrow$ $\delta \approx 0.4$

$(g_K - g_R) \approx 1.4$ for [202 5/2] etc.

ex. $^{11}_{4}Be_{7}$ (N = 7)

S_n = 504 keV

½ - —— 319.8

½ + —— 0 (i.e. neutron binding energy = 504 keV)

The observed spectra can be easily understood if the deformation δ ~ 0.6 . Indeed, the observed deformation in ^{12}Be(p,p') is β ~ 0.7 .

N=8 is not a magic number !

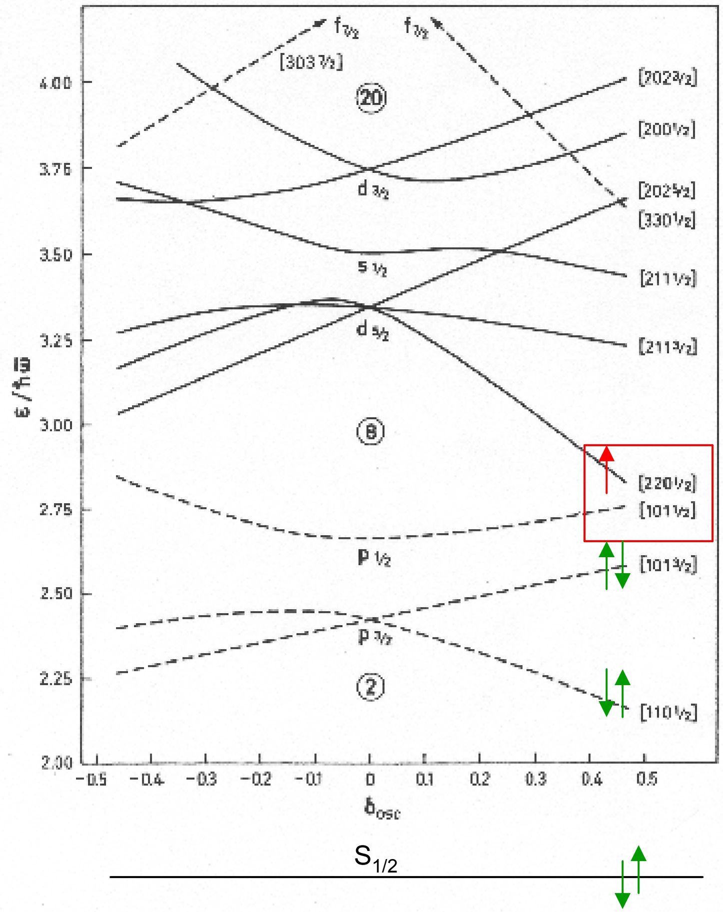

An additional element :

weakly-bound [220 ½]

→ major component becomes $s_{1/2}$ (halo)

→ one-particle energy is pushed down relative to $p_{1/2}$

In the spherical shell-model the above ½+ state must be interpreted as the 1-particle (in the *sd*-shell) 2-hole (in the *p*-shell) state, which was pushed down below the ½- state (1-hole in the *p*-shell) due to some residual interaction.

Table 1.

Selection rule of one-particle operators between one-particle states with exact quantum numbers $(N\ n_z\ \Lambda\ \Omega)$.

Matrix elements of the most important operators in the asymptotic basis, and their selection rules

Operator O	ΔN	ΔN_z	$\Delta \Lambda$	$\Delta \Sigma$	$\Delta \Omega$	$\langle N'N'_z\Lambda'\|O\|NN_z\Lambda\rangle$
$l_t \cdot s$	0	0	0	0	0	$\Lambda\Sigma$
	0	1	±1	∓1	0	$-\frac{1}{2}(\frac{1}{2}\pm\Sigma)\,[(N_z+1)\,(N-N_z\mp\Lambda)]^{\frac{1}{2}}$
	0	-1	±1	∓1	0	$-\frac{1}{2}(\frac{1}{2}\pm\Sigma)\,[N_z\,(N-N_z\pm\Lambda+2)]^{\frac{1}{2}}$
l_t^2	0	0	0	0	0	$\Lambda^2+\Lambda+2\,[N_z\,(N-N_z+1)]+(N-N_z-\Lambda)$
	0	2	0	0	0	$[(N_z+1)\,(N_z+2)\,(N-N_z+\Lambda)\,(N-N_z-\Lambda)]^{\frac{1}{2}}$
	0	-2	0	0	0	$[N_z\,(N_z-1)\,(N-N_z\mp\Lambda+2)\,(N-N_z-\Lambda+2)]^{\frac{1}{2}}$
z'	±1	±1	0	0	0	$c_z\,[\frac{1}{2}(N_z\,\mathrm{sup})]^{\frac{1}{2}}$
$x'\pm iy'$	$+1$	0	±1	0	±1	$\pm c_\perp\,[\frac{1}{2}(N-N_z\pm\Lambda+2)]^{\frac{1}{2}}$
	-1	0	±1	0	±1	$\mp c_\perp\,[\frac{1}{2}(N-N_z\mp\Lambda)]^{\frac{1}{2}}$
z'^2	0	0	0	0	0	$c_z^2\,(N_z+\frac{1}{2})$
	2	2	0	0	0	$\frac{1}{2}c_z^2\,[(N_z+1)\,(N_z+2)]^{\frac{1}{2}}$
	-2	-2	0	0	0	$\frac{1}{2}c_z^2\,[N_z\,(N_z-1)]^{\frac{1}{2}}$
$x'^2+y'^2$	0	0	0	0	0	$c_\perp^2\,(N-N_z+1)$
	2	0	0	0	0	$-\frac{1}{2}c_\perp^2\,[(N-N_z+\Lambda+2)\,(N-N_z-\Lambda+2)]^{\frac{1}{2}}$
	-2	0	0	0	0	$-\frac{1}{2}c_\perp^2\,[(N-N_z+\Lambda)\,(N-N_z-\Lambda)]^{\frac{1}{2}}$
$z'(x'\pm iy')$	0	1	±1	0	±1	$\mp\frac{1}{2}c_\perp c_z\,[(N_z+1)\,(N-N_z\mp\Lambda)]^{\frac{1}{2}}$
	0	-1	±1	0	±1	$\pm\frac{1}{2}c_\perp c_z\,[N_z\,(N-N_z\pm\Lambda+2)]^{\frac{1}{2}}$
	2	1	±1	0	±1	$\pm\frac{1}{2}c_\perp c_z\,[(N_z+1)\,(N-N_z\pm\Lambda+2)]^{\frac{1}{2}}$
	-2	-1	±1	0	±1	$\mp\frac{1}{2}c_\perp c_z\,[N_z\,(N-N_z\mp\Lambda)]^{\frac{1}{2}}$
$(x'\pm iy')^2$	0	0	±2	0	±2	$-c_\perp^2\,[(N-N_z\mp\Lambda)\,(N-N_z\pm\Lambda+2)]^{\frac{1}{2}}$
	2	0	±2	0	±2	$\frac{1}{2}c_\perp^2\,[(N-N_z\pm\Lambda+2)\,(N-N_z\pm\Lambda+4)]^{\frac{1}{2}}$
	-2	0	±2	0	±2	$\frac{1}{2}c_\perp^2\,[(N-N_z\mp\Lambda)\,(N-N_z\mp\Lambda-2)]^{\frac{1}{2}}$
l_z	0	0	0	0	0	Λ
$l_x\pm il_y$	0	1	±1	0	±1	$-\mathscr{S}\,[(N_z+1)\,(N-N_z\mp\Lambda)]^{\frac{1}{2}}$
	0	-1	±1	0	±1	$-\mathscr{S}\,[N_z\,(N-N_z\pm\Lambda+2)]^{\frac{1}{2}}$
	2	1	±1	0	±1	$\mathscr{D}\,[(N_z+1)\,(N-N_z\pm\Lambda+2)]^{\frac{1}{2}}$
	-2	-1	±1	0	±1	$\mathscr{D}\,[N_z\,(N-N_z\mp\Lambda)]^{\frac{1}{2}}$
s_z	0	0	0	0	0	Σ
$s_x\pm is_y$	0	0	0	±1	±1	$[(\frac{1}{2}\mp\Sigma)\,(\frac{1}{2}\pm\Sigma+1)]^{\frac{1}{2}}$

The matrix elements between the levels with the assigned asymptotic quantum numbers, $[N\ n_z\ \Lambda\ \Omega]$, can be obtained, to leading order, from this table.

E1 operator

E2 operator

M1 operator

Gamow-Teller operator

From J.P.Boisson and R.Piepenbring, Nucl. Phys. A168(1971)385.

If you use this kind of tables, you must be careful about the sign of the non-diagonal matrix elements, which depends on the phase convention of wave functions !

Table 2.

$$\left|(\ell s)j,\Omega\right\rangle \equiv \frac{1}{r}R_{\ell j}(r)\sum_{m_\ell m_s} C(\ell,1/2,j;m_\ell m_s\Omega)Y_{\ell m_\ell}(\theta,\phi)\chi_{1/2,m_s}$$

$$\left\langle \ell_2 j_2\left|r^\lambda\right|\ell_1 j_1\right\rangle \equiv \int_0^\infty dr R_{\ell_2 j_2}(r)R_{\ell_1 j_1}(r)r^\lambda$$

Matrix-elements of one-particle operators in $|(\ell\, s)\, j,\, \Omega\rangle$ representations

$$\left\langle (\ell_2 s)j_2,\Omega\left|r^\lambda Y_{\lambda 0}\right|(\ell_1 s)j_1,\Omega\right\rangle$$
$$= \delta\left((-1)^{\ell_1+\ell_2},(-1)^\lambda\right)\left\langle \ell_2 j_2\left|r^\lambda\right|\ell_1 j_1\right\rangle(-1)^{j_1+j_2+1+\lambda}(-1)^{\Omega-\frac{1}{2}}\sqrt{\frac{(2j_1+1)(2j_2+1)}{4\pi(2\lambda+1)}}$$
$$C(j_2 j_1\lambda;1/2,-1/2,0)\;\; C(j_2 j_1\lambda;\Omega,-\Omega,0)$$

$$\left\langle (\ell_2 s)j_2,\Omega+1\left|r^\lambda Y_{\lambda 1}\right|(\ell_1 s)j_1,\Omega\right\rangle$$
$$= \delta\left((-1)^{\ell_1+\ell_2},(-1)^\lambda\right)\left\langle \ell_2 j_2\left|r^\lambda\right|\ell_1 j_1\right\rangle(-1)^{j_1+j_2+1+\lambda}(-1)^{\Omega-1/2}\sqrt{\frac{(2j_1+1)(2j_2+1)}{4\pi(2\lambda+1)}}$$
$$C(j_2 j_1\lambda;1/2,-1/2,0)\;\; C(j_2 j_1\lambda;\Omega+1,-\Omega,1)$$
$$= (-1)\left\langle (\ell_1 s)j_1,\Omega\left|r^\lambda Y_{\lambda -1}\right|(\ell_2 s)j_2,\Omega+1\right\rangle$$

$$\left\langle (\ell_2 s)j_2,\Omega+2\left|r^\lambda Y_{\lambda 2}\right|(\ell_1 s)j_1,\Omega\right\rangle$$
$$= \delta\left((-1)^{\ell_1+\ell_2},(-1)^\lambda\right)\left\langle \ell_2 j_2\left|r^\lambda\right|\ell_1 j_1\right\rangle(-1)^{j_1+j_2+1+\lambda}(-1)^{\Omega-1/2}\sqrt{\frac{(2j_1+1)(2j_2+1)}{4\pi(2\lambda+1)}}$$
$$C(j_2 j_1\lambda;1/2,-1/2,0)\;\; C(j_2 j_1\lambda;\Omega+2,-\Omega,2)$$
$$= \left\langle (\ell_1 s)j_1,\Omega\left|r^\lambda Y_{\lambda -2}\right|(\ell_2 s)j_2,\Omega+2\right\rangle$$

Table 2 (continued) ($s_\pm = s_x \pm i\, s_y$ etc.)

$$\langle \ell_2 j_2 | \ell_1 j_1 \rangle \equiv \int_0^\infty dr R_{\ell_2 j_2}(r) R_{\ell_1 j_1}(r)$$

$$\langle (\ell_2 s) j_2, \Omega+1 | s_+ | (\ell_1 s) j_1, \Omega \rangle$$

$$= \delta(\ell_1, \ell_2)(-1)^{\ell_1 + j_1 + 1/2} \sqrt{3(2 j_1 + 1)} \;\; C(j_1, 1, j_2; \Omega, 1, \Omega+1) \;\; W(1/2, j_2, 1/2, j_1; \ell_1 1) \; \langle \ell_2 j_2 | \ell_1 j_1 \rangle$$

$$\langle (\ell_2 s) j_2, \Omega+1 | \ell_+ | (\ell_1 s) j_1, \Omega \rangle$$

$$= \delta(\ell_1, \ell_2)(-1)^{\ell_1 + j_2 - 1/2} \sqrt{2(2 j_1 + 1)} \sqrt{\ell_1(\ell_1+1)(2\ell_1+1)} \;\; C(j_1 1 j_2; \Omega, 1, \Omega+1) \;\; W(\ell_2 j_2 \ell_1 j_1; 1/2, 1)$$

$$\langle \ell_2 j_2 | \ell_1 j_1 \rangle$$

$$\langle (\ell_2 s) j_2, \Omega+1 | j_+ | (\ell_1 s) j_1, \Omega \rangle = \delta(j_1, j_2) \sqrt{(j - \Omega)(j + \Omega + 1)} \;\; \langle \ell_2 j_2 | \ell_1 j_1 \rangle$$

$$\langle (\ell_2 s) j_2, \Omega | s_z | (\ell_1 s) j_1, \Omega \rangle$$

$$= \delta(\ell_1, \ell_2)(-1)^{\ell_1 + j_1 - 1/2} \sqrt{\frac{3(2 j_1 + 1)}{2}} \;\; C(j_1, 1, j_2; \Omega, 0, \Omega) \;\; W(1/2, j_2, 1/2, j_1; \ell_1 1) \;\; \langle \ell_2 j_2 | \ell_1 j_1 \rangle$$

$$\langle (\ell_2 s) j_2, \Omega | \ell_z | (\ell_1 s) j_1, \Omega \rangle$$

$$= \delta(\ell_1, \ell_2)(-1)^{\ell_1 + j_2 + 1/2} \sqrt{2 j_1 + 1} \sqrt{\ell_1(\ell_1+1)(2\ell_1+1)} \;\; C(j_1 1 j_2; \Omega 0 \Omega) \;\; W(\ell_2 j_2 \ell_1 j_1; 1/2, 1)$$

$$\langle \ell_2 j_2 | \ell_1 j_1 \rangle$$

Table 2 (continued)

Phase convention in wave functions - important in non-diagonal matrix-elements

1) (ℓs)j or (sℓ)j ; $\quad |(s\ell)\,j\rangle = (-1)^{\frac{1}{2}+\ell-j}|(\ell s)\,j\rangle$

2) $Y_{\ell m_\ell}(\theta,\phi)$ or $i^{\ell} Y_{\ell m_\ell}(\theta,\phi)$

3) $R_{\ell j}(r)$ $\left\{ \begin{array}{l} > 0 \text{ (or } < 0) \quad \text{for } r \rightarrow 0, \quad \text{or} \\ > 0 \text{ (or } < 0) \quad \text{for } r \rightarrow \text{very large}, \quad \text{or} \\ \text{output of computers} \end{array} \right.$

5. Weakly-bound and one-particle resonant neutron levels in Y20 deformed potential

~~harmonic-oscillater potential~~

Well-bound one-particle levels in deformed potential

A.Bohr and B.R.Mottelson, vol.2, Figure 5-1.

One-particle levels in (Y_{20}) deformed harmonic oscillator potentials

$[N\, n_z\, \Lambda\, \Omega\,]$

asymptotic quantum numbers

Parity $\pi = (-1)^N$

Each levels are doubly-degenerate with $\pm\Omega$

6 doubly-degenerate levels in sd-shell

3 $\Omega^\pi = 1/2^+$ ($\ell_{min}=0$)
2 $\Omega^\pi = 3/2^+$ ($\ell_{min}=2$)
1 $\Omega^\pi = 5/2^+$ ($\ell_{min}=2$)
} 12 particles

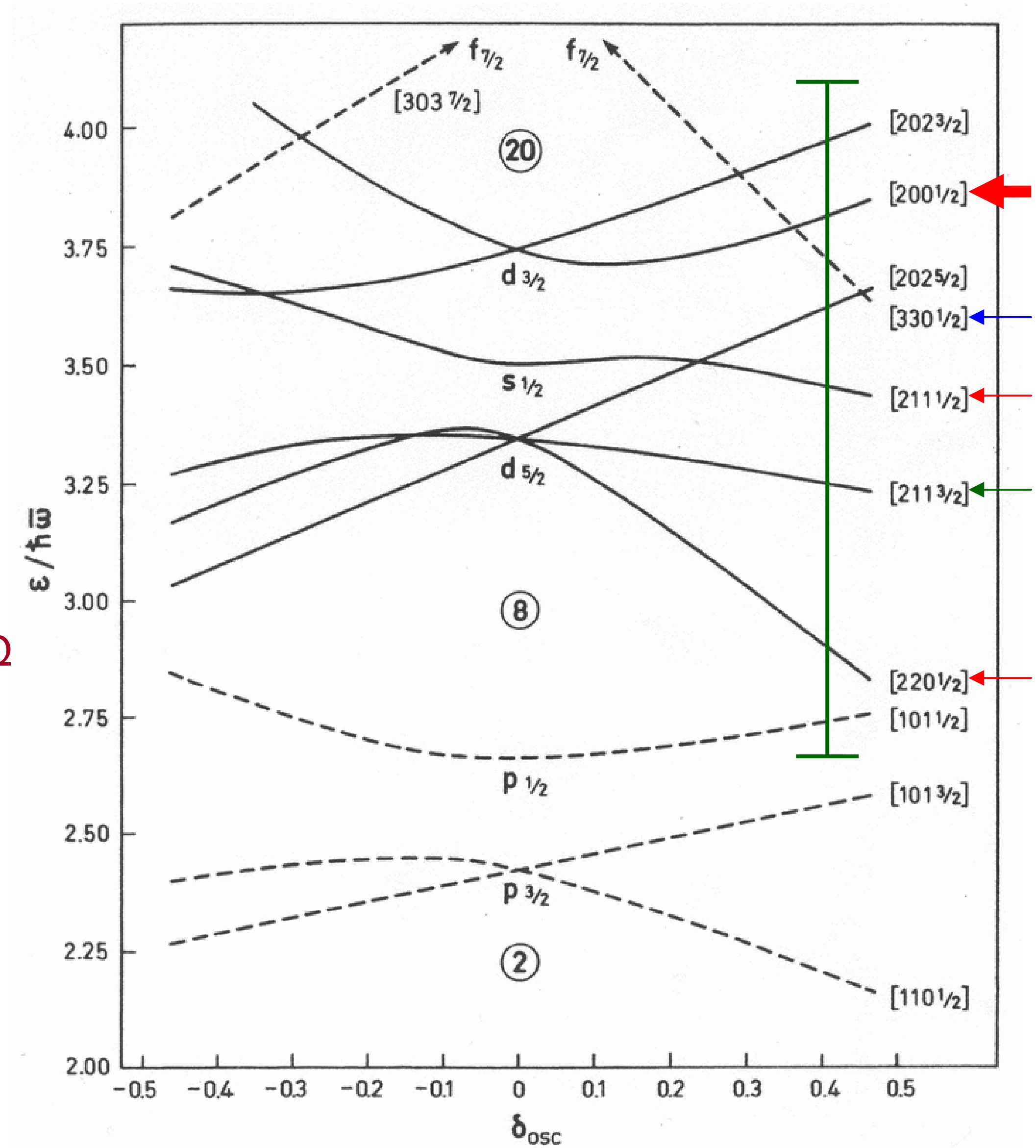

5.1. Weakly-bound neutrons

Radial wave functions of the [200 ½] level
in Woods-Saxon potentials

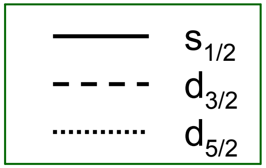

(The radius of potentials is adjusted to obtain respective eigenvalues ε_Ω .)

Bound state with ε_Ω = -8.0 MeV.

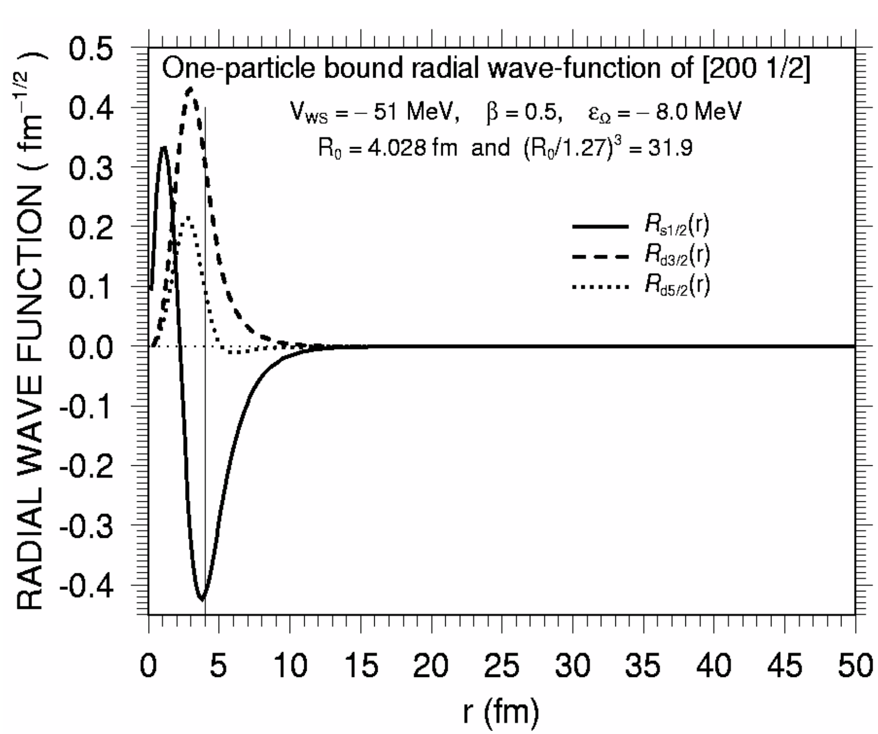

Similar behavior to wave functions in harmonic osc. potentials.

Bound state with ε_Ω = -0.0001 MeV.

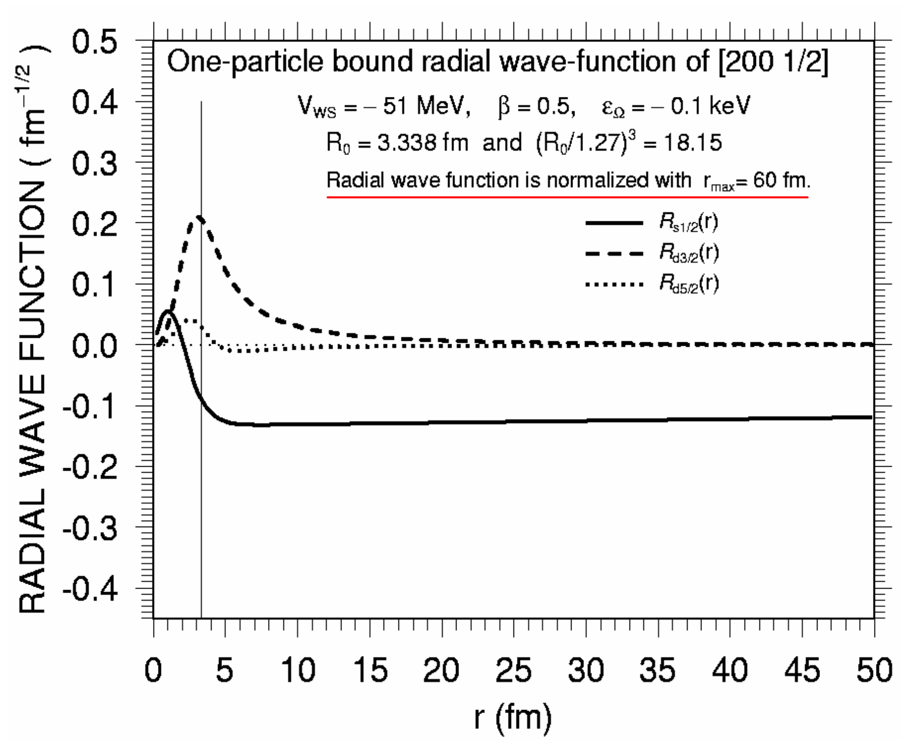

Wave functions unique in finite-well potentials.

W-S potential parameters are fixed except radius *R*.

I.H., Phys. Rev. **C72**, 024301 (2005)

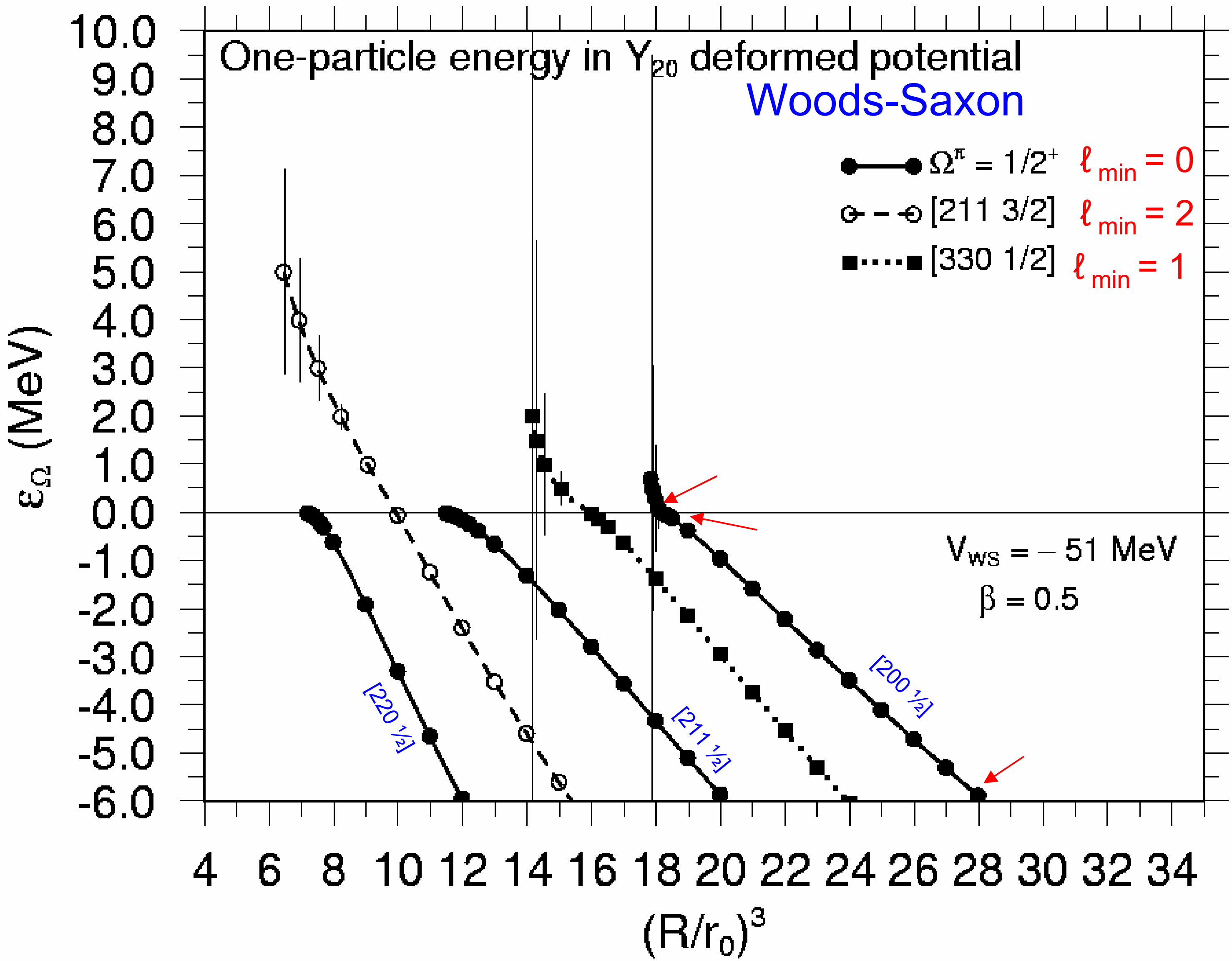

potential strength

(r_0 = 1.27 fm is used.)

PRC**69**, 041306R (2004)

Deformed halo nuclei

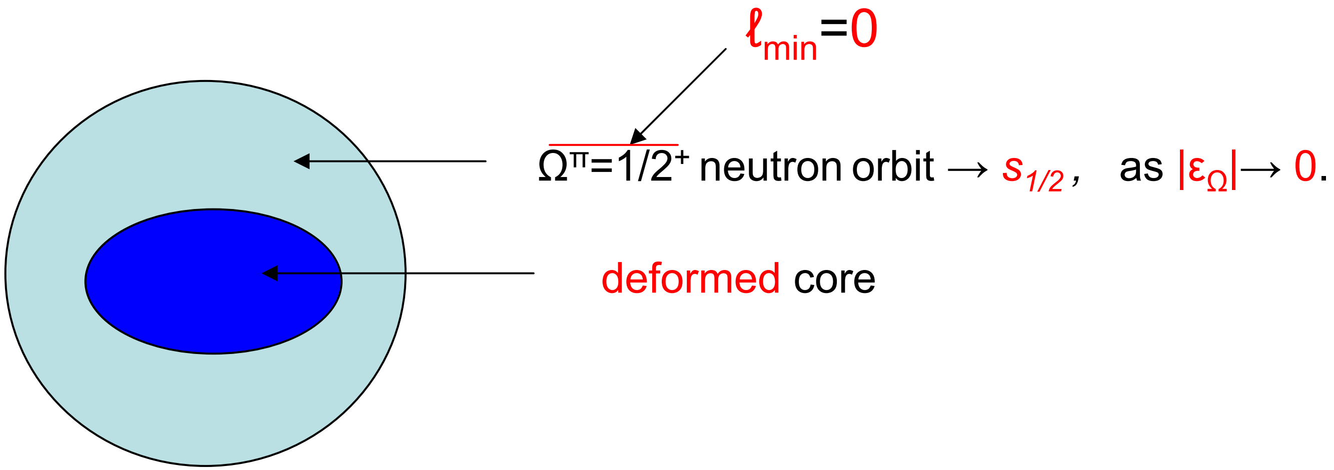

, irrespective of the size of deformation and the kind of one-particle orbits.

The rotational spectra of deformed halo nuclei must come from the deformed core.

For $\varepsilon \to 0$, the *s*-dominance will appear in all $\Omega^\pi = 1/2^+$ bound orbits. However, the energy, at which the dominance shows up, depends on both deformation and respective orbits.

ex. three $\Omega^\pi = 1/2^+$ Nilsson orbits in the *sd*-shell ;

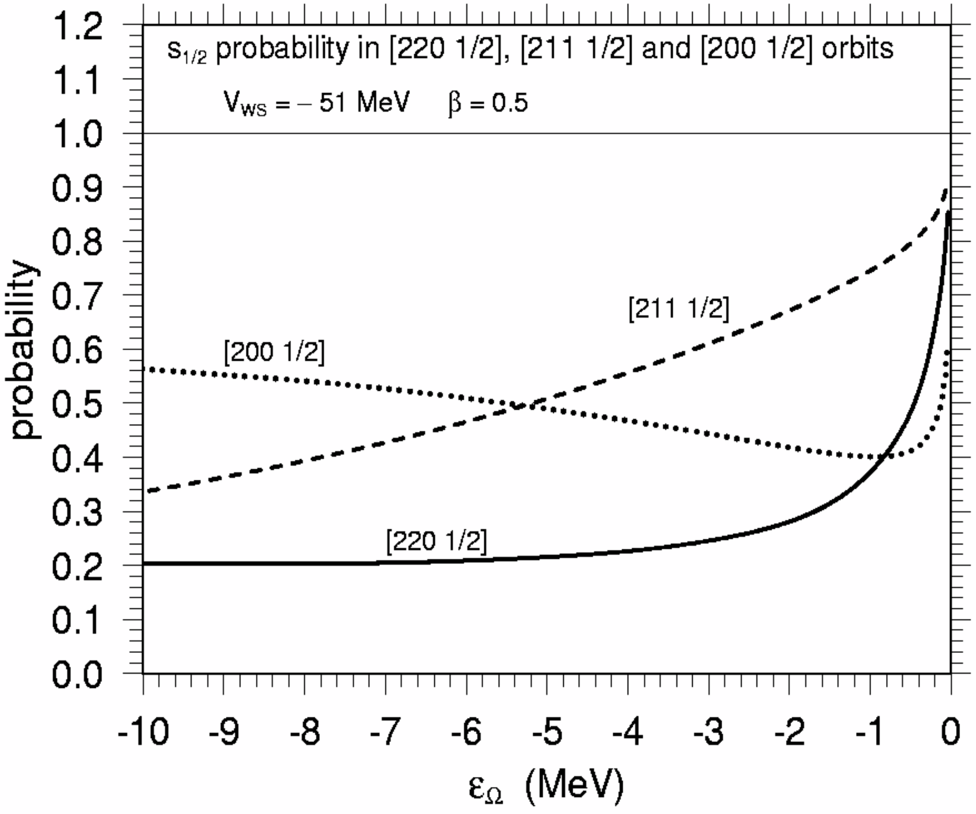

5.2. One-particle resonant levels – eigenphase formalism

Radial wave functions of the [200 ½] level

—— $s_{1/2}$ - - - - $d_{3/2}$ .... $d_{5/2}$

The potential radius is adjusted to obtain respective eigenvalue ($\varepsilon_\Omega < 0$) and resonance ($\varepsilon_\Omega > 0$).

Resonant state with ε_Ω = +100 keV

Bound state with ε_Ω = – 0.1 keV

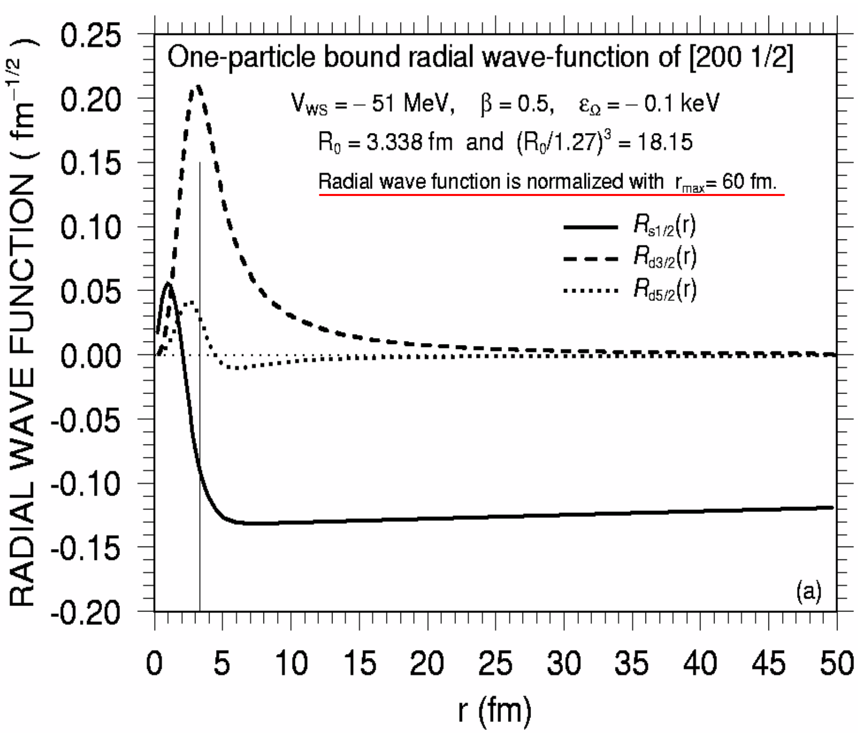

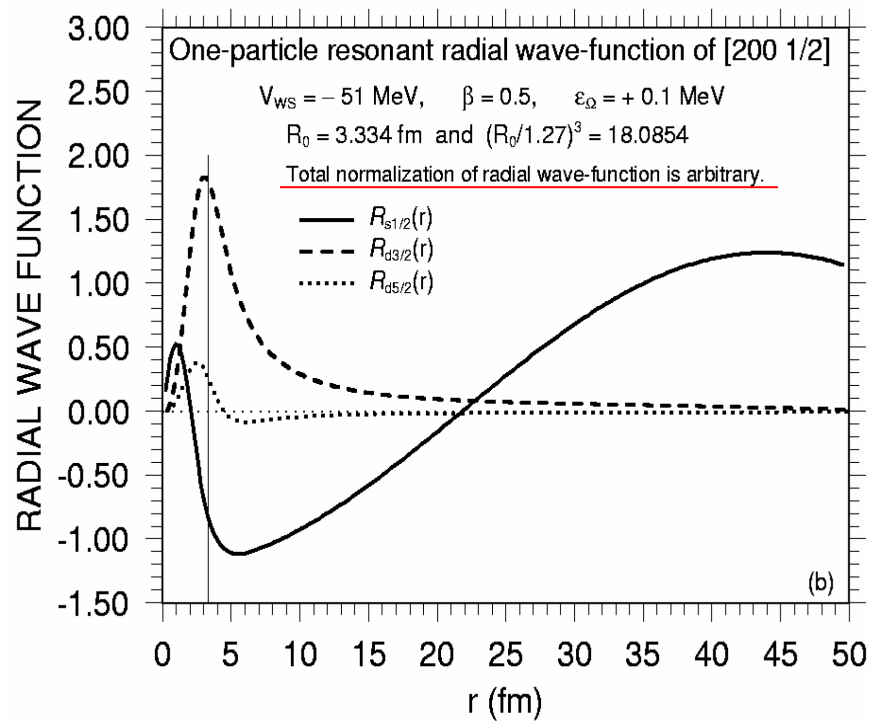

Existence of resonance ← d component

Width of resonance ← s component

OBS. Relative amplitudes of various components inside the potential remain nearly the same for ε_Ω = – 0.1 keV ⟶ + 100 keV.

Relative probability of $s_{1/2}$ component inside the W-S potential

$$P(s_{1/2}) = \frac{\langle s_{1/2} | V(r) | s_{1/2} \rangle}{\langle d_{5/2} | V(r) | d_{5/2} \rangle + \langle d_{3/2} | V(r) | d_{3/2} \rangle + \langle s_{1/2} | V(r) | s_{1/2} \rangle}$$

In order that one-particle resonance continues for $\varepsilon_\Omega > 0$,
$P(s_{1/2})$ at $\varepsilon_\Omega = 0$ must be smaller than some critical value.
The critical value depends on the diffuseness of the potential.

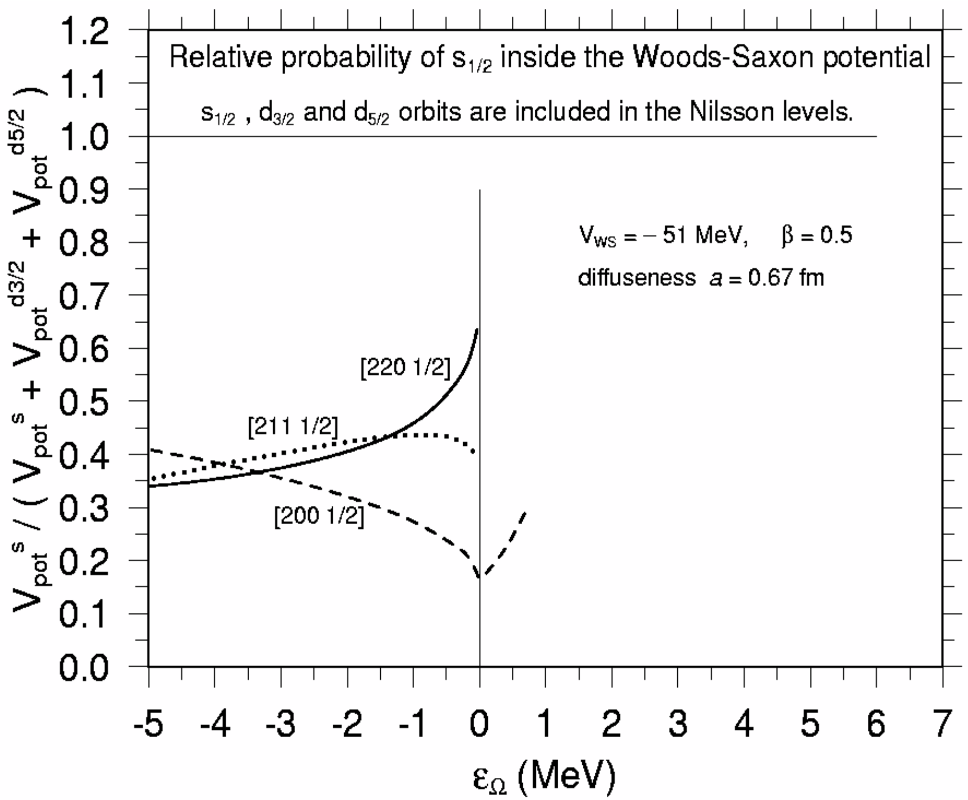

One-particle shell-structure change for ε_Ω (<0) → 0 produces the large change of $P(s_{1/2})$ values of respective $[N\, n_z\, \Lambda\, \Omega]$ orbits as ε_Ω (<0) → 0.

→ One-particle resonance

Positive-energy neutron levels in Y_{20}-deformed potentials

$\Omega^\pi = 1/2^+$ $s_{1/2}$, $d_{3/2}$, $d_{5/2}$, $g_{7/2}$,$g_{9/2}$, ….., components $\ell_{min} = 0$

$\Omega^\pi = 3/2^+$ $d_{3/2}$, $d_{5/2}$, $g_{7/2}$, $g_{9/2}$, ….., components $\ell_{min} = 2$

$\Omega^\pi = 1/2^-$ $p_{1/2}$, $p_{3/2}$, $f_{5/2}$, $f_{7/2}$, $h_{9/2}$, ….., components $\ell_{min} =1$

etc.

The component with $\ell = \ell_{min}$ plays a crucial role in the properties of possible one-particle resonant levels.

(Among an infinite number of positive-energy one-particle levels, one-particle resonant levels are most important in the construction of many-body correlations of nuclear bound states.)

Do not restrict the system in a finite box !

For $\varepsilon_\Omega < 0$

$$R_{\ell j\Omega}(r) \propto r h_\ell(\alpha_b r) \qquad \text{for} \qquad r \to \infty$$

where

$$h_\ell(-iz) \equiv j_\ell(z) + i n_\ell(z) \qquad \text{and} \qquad \alpha_b^2 \equiv -\frac{2m\varepsilon_\Omega}{\hbar^2}$$

For $\varepsilon_\Omega > 0$

$$R_{\ell j\Omega}(r) \propto \cos(\delta_\Omega) r j_\ell(\alpha_c r) - \sin(\delta_\Omega) r n_\ell(\alpha_c r) \qquad \text{for} \qquad r \to \infty$$

$$\to \sin(\alpha_c r + \delta_\Omega - \ell \frac{\pi}{2})$$

where

$$\alpha_c^2 \equiv \frac{2m}{\hbar^2}\varepsilon_\Omega$$

δ_Ω expresses eigenphase.

A.U.Hazi, Phys.Rev.A19, 920 (1979).

K.Hagino and Nguyen Van Giai, Nucl.Phys.A735, 55 (2004).

A given eigenchannel : asymptotic radial wave-functions behave in the same way for all angular momentum components.

A one-particle resonant level with ε_Ω is defined so that one eigenphase δ_Ω increases through $(1/2)\pi$ as ε_Ω increases.

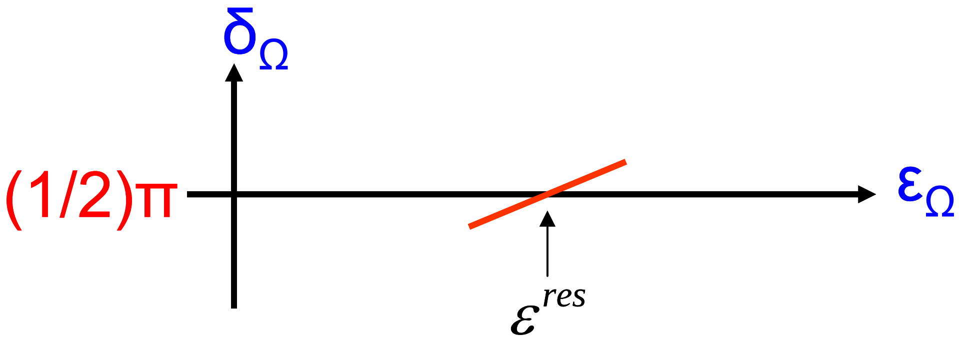

When one-particle resonant level in terms of one eigenphase is obtained, the width Γ of the resonance is calculated by

$$\Gamma \equiv \frac{2}{\left[\dfrac{d\delta_\Omega}{d\varepsilon_\Omega}\right]_{\varepsilon_\Omega=\varepsilon_\Omega^{res}}}$$

Phys. Rev. C72, 024301 2005)

I.H., Phys. Rev. C73, 064308 (2006)

Some comments on eigenphase ;

1) For a given potential and a given ε_Ω
there are several (in principle, an infinite number of) solutions of eigenphase δ_Ω .

2) The number of eigenphases for a given potential and a given ε_Ω is equal to that of wave function components with different (ℓ,j) values.

3) The value of δ_Ω determines the relative amplitudes of different (ℓ,j) components.

4) In the region of small values of ε_Ω (> 0), only one of eigenphases varies strongly as a function of ε_Ω , while other eigenphases remain close to the values of $n\pi$.

In the limit of $\beta\rightarrow 0$, the definition of one-particle resonance in eigenphase formalism
→ the definition in spherical potentials found in text books.

Variation of all three eigenphases
($s_{1/2}$, $d_{3/2}$ and $d_{5/2}$ levels are included in the coupled channels.)

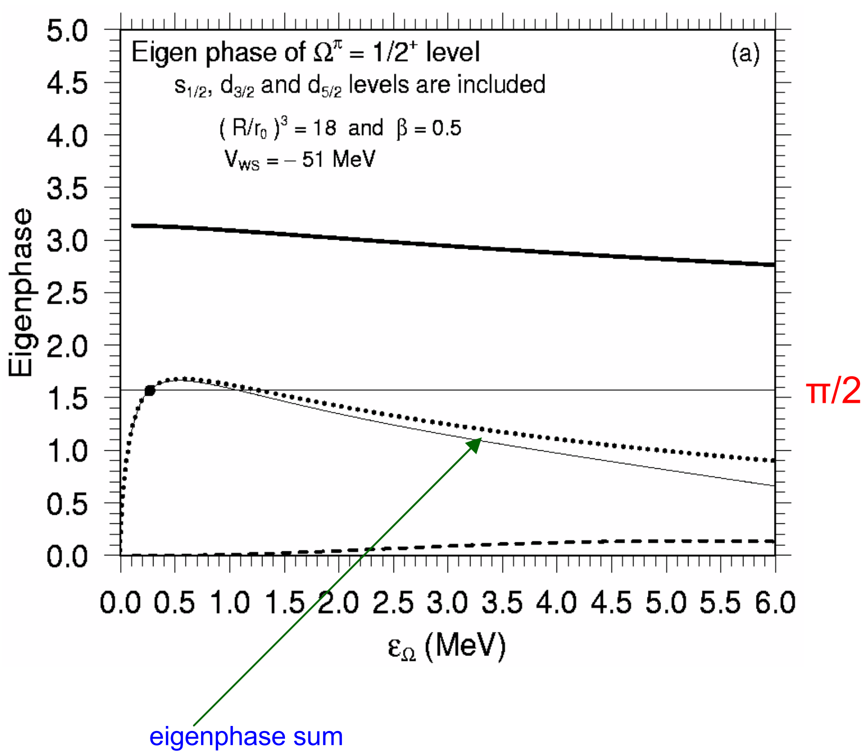

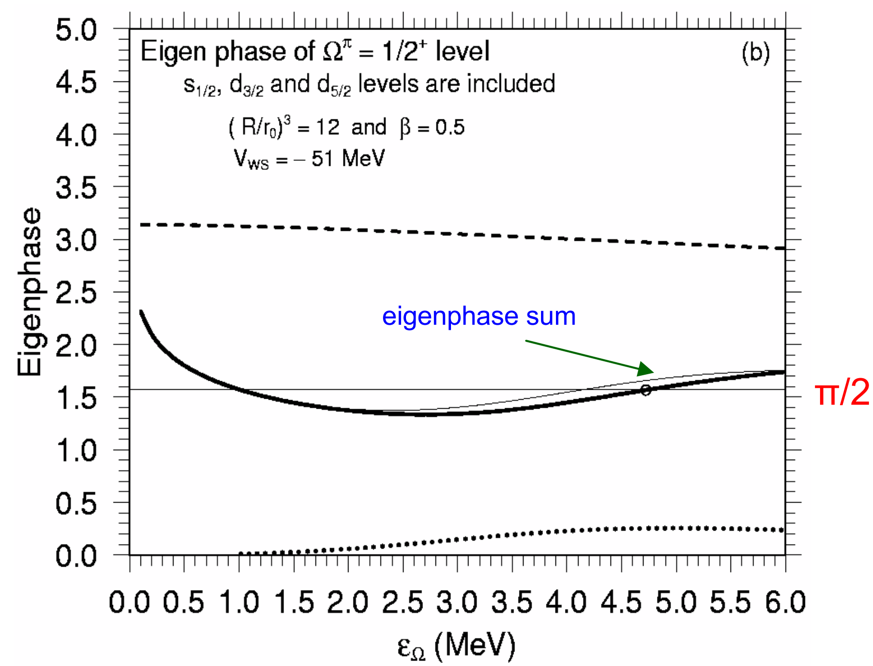

No weakly-bound Nilsson level is present for this potential.

A weakly-bound Nilsson level is present for this potential.

5.3. Examples of Nilsson diagrams for light neutron-rich nuclei

1. ~ $^{17}C_{11}$ ($S(n) = 0.73$ MeV, $3/2^+$)

2. ~ $^{31}Mg_{19}$ ($S(n) = 2.38$ MeV, $1/2^+$)

   ~ $^{33}Mg_{21}$ ($S(n) = 2.22$ MeV, $3/2^-$)

Near degeneracy of some weakly-bound or resonant levels in spherical potential, unexpected from the knowledge on stable nuclei

- the origin of deformation and …….

  Jahn-Teller effect

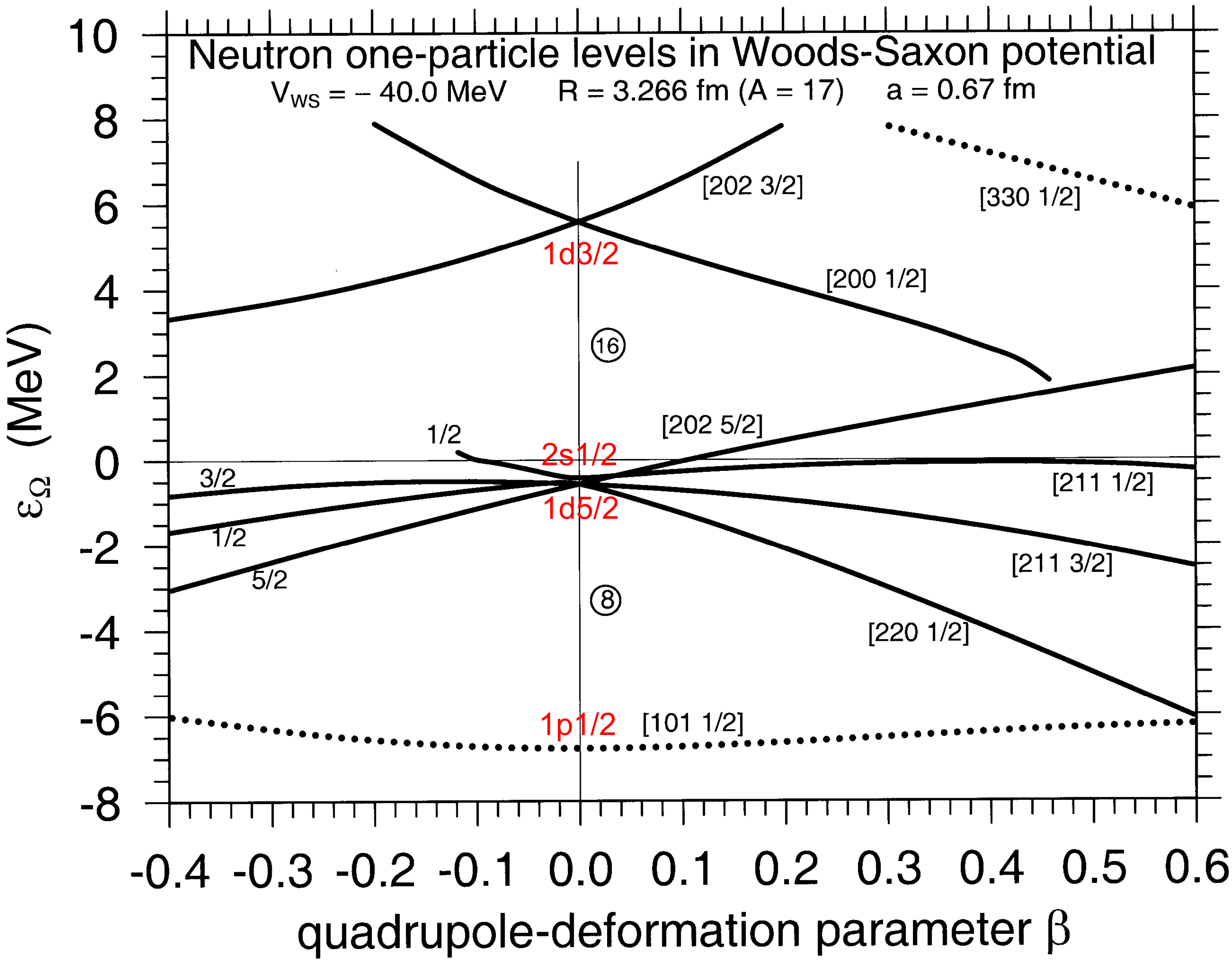

At $\beta=0$;
$\varepsilon(2s1/2)-\varepsilon(1d5/2)$
= 140 keV

$^{17}C_{11}$ (3/2+)

S(n) = 0.73 MeV

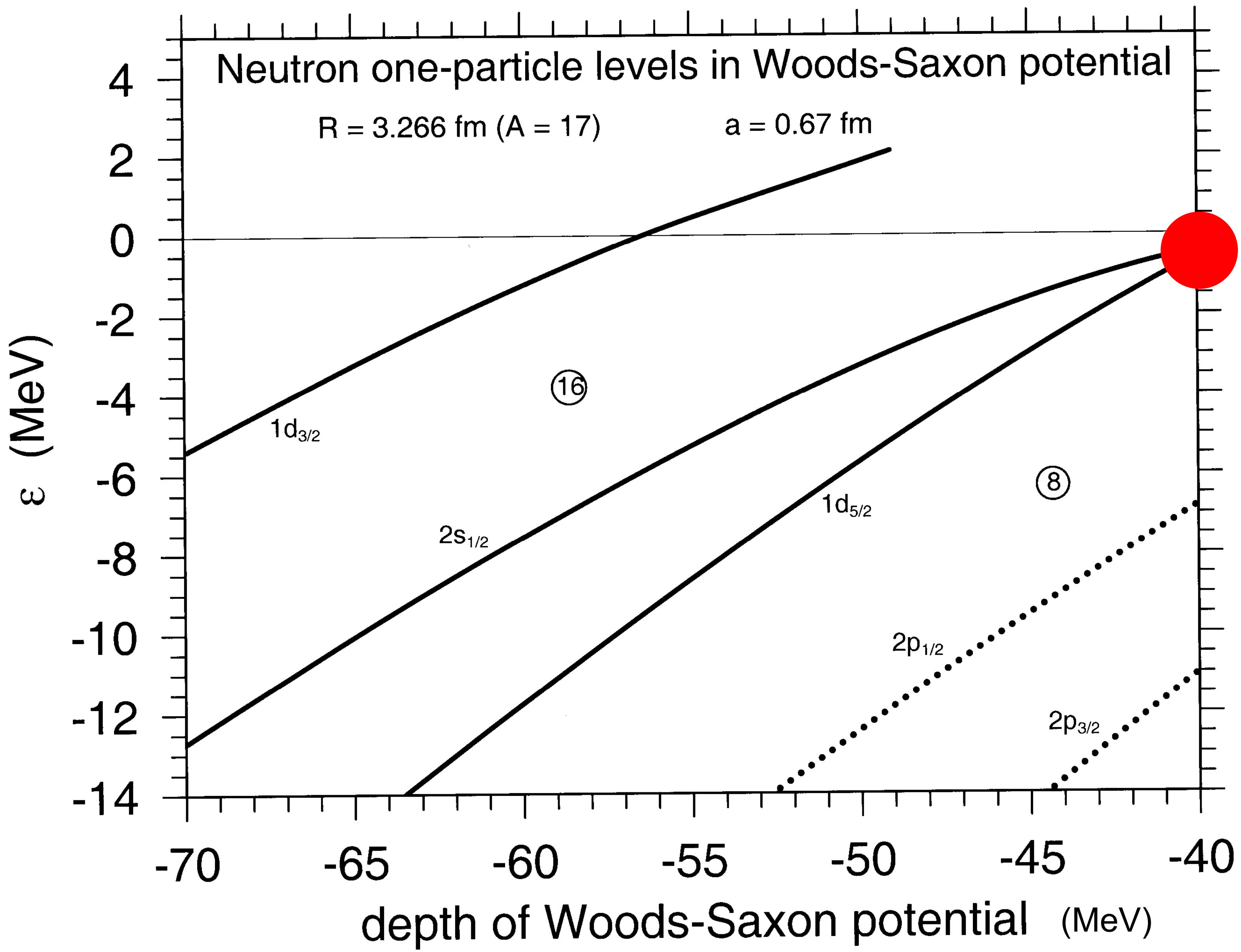

Neutron one-particle levels in Woods-Saxon potential
R = 3.266 fm (A = 17)
a = 0.67 fm
4
2
0
-2
-4
-6
-8
-10
-12
-14
ε (MeV)
1d3/2
16
2s1/2
1d5/2
8
2p1/2
2p3/2
-70
-65
-60
-55
-50
-45
-40
depth of Woods-Saxon potential (MeV)

$\varepsilon(1f_{5/2}) = +8.96$ MeV

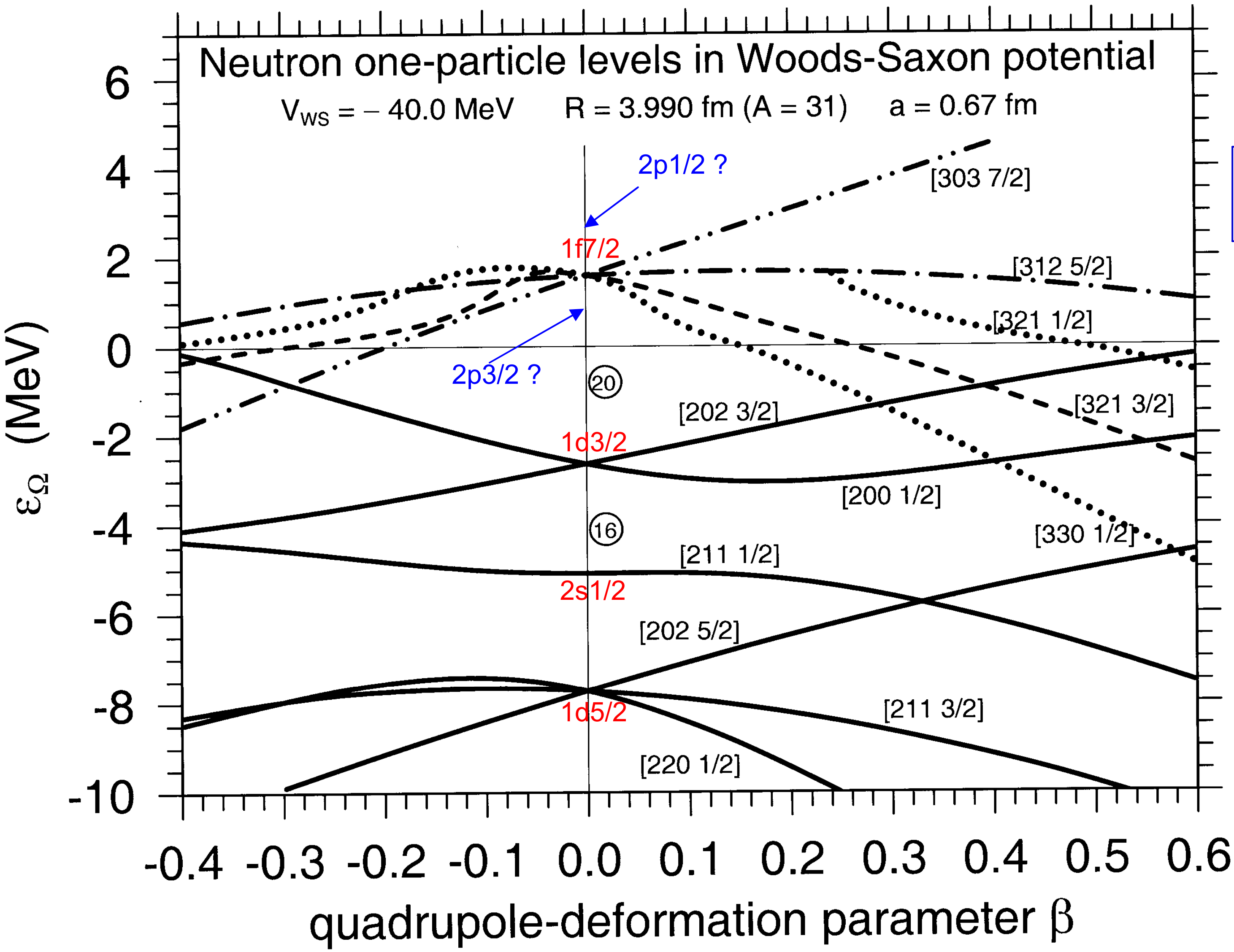

At $\beta=0$;
$\varepsilon(2p3/2) < \varepsilon(1f7/2)$

$^{33}Mg_{21}$ (3/2–)
S(n) = 2.22 MeV

$^{31}Mg_{19}$ (1/2+)
S(n) = 2.38 MeV

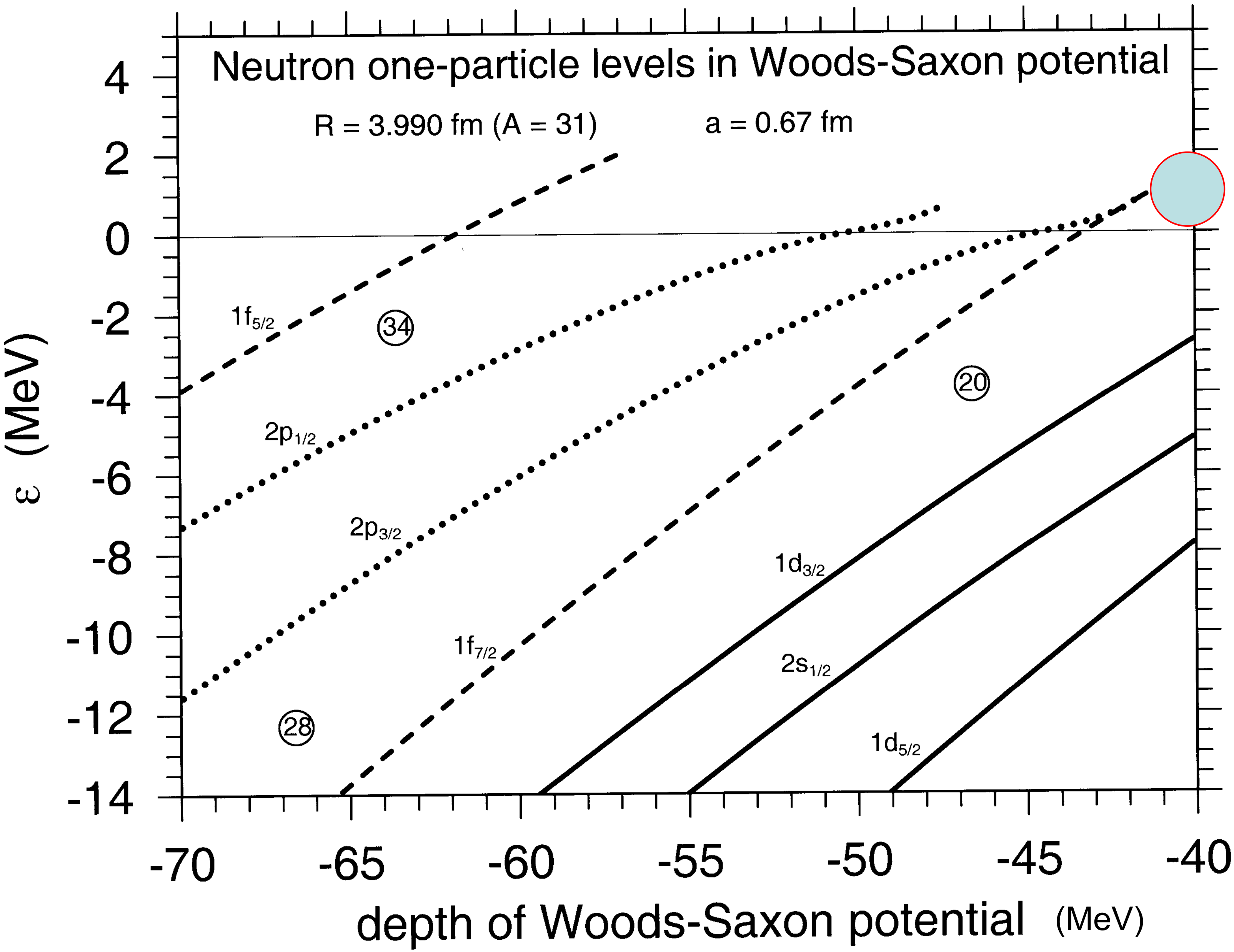
Neutron one-particle levels in Woods-Saxon potential
R = 3.990 fm (A = 31)
a = 0.67 fm
1f5/2
34
2p1/2
2p3/2
20
1d3/2
1f7/2
2s1/2
28
1d5/2
ε (MeV)
4
2
0
-2
-4
-6
-8
-10
-12
-14
-70
-65
-60
-55
-50
-45
-40
depth of Woods-Saxon potential (MeV)

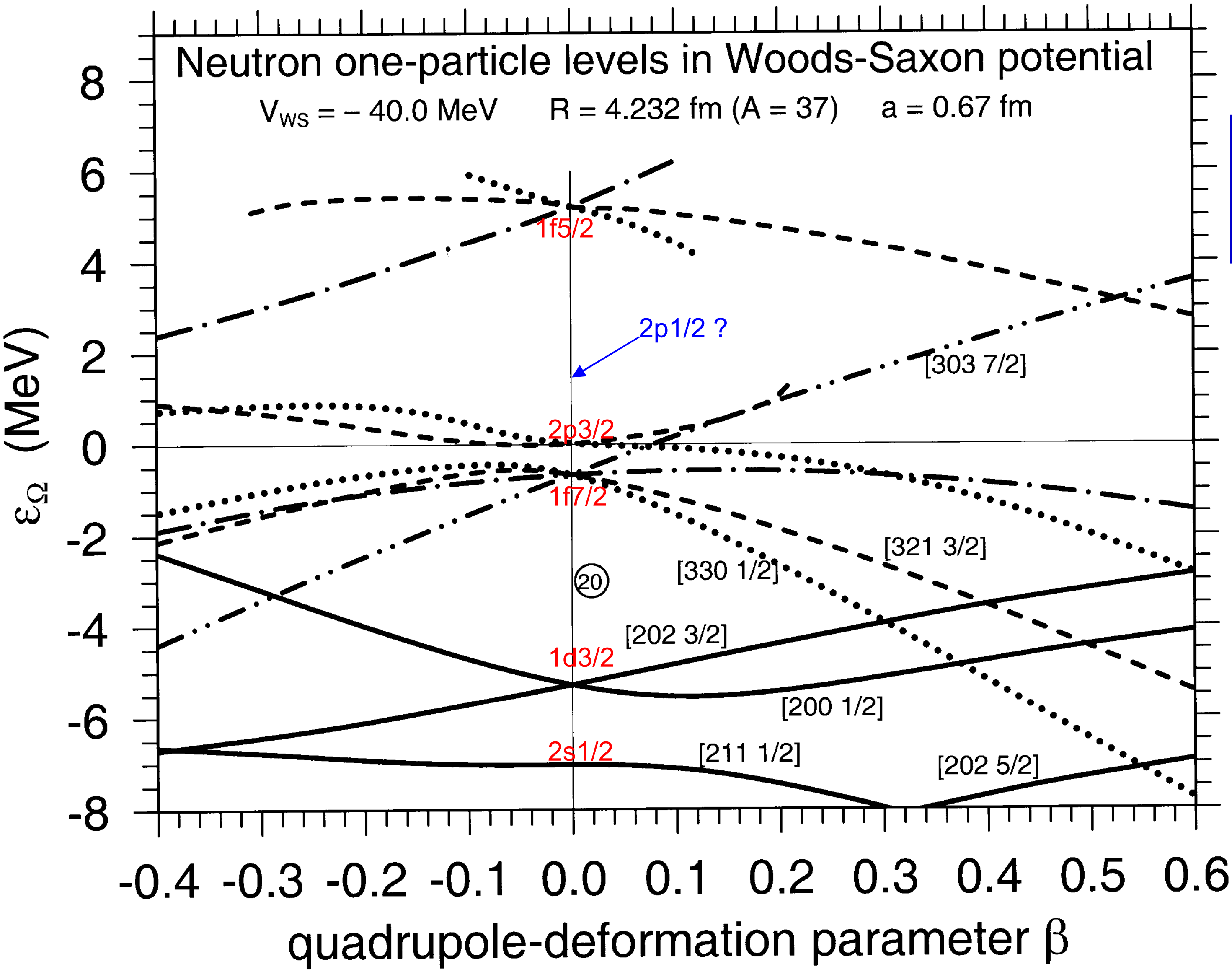

At $\beta=0$;
ε(2p3/2) – ε(1f7/2)
= 680 keV

$^{37}Mg_{25}$

S(n) = a few hundreds keV ?

Appendix. Angular momentum projection from a deformed intrinsic state $|\phi\rangle$

(ex. not appropriate for including the rotational perturbation of intrinsic states)

Rotational operator $R(\Omega)$ Ω : Euler angles (α, β, γ)

$$R(\Omega) \equiv e^{-i\alpha J_z} e^{-i\beta J_y} e^{-i\gamma J_z}$$

Rotation matrix $D^J_{MM'}(\Omega)$

$$\langle \alpha JM | R(\Omega) | \alpha' J' M' \rangle = \delta(\alpha, \alpha')\delta(J, J') D^J_{MM'}(\Omega)$$

Inverting the expression

$$R(\Omega) = \sum_{\alpha J} | \alpha JM \rangle D^J_{MM'}(\Omega) \langle \alpha JM' |$$

Multiplying by $D^J_{MM'}{}^*(\Omega)$ and integrating over Ω, we obtain a projection operator

$$P^J_M \equiv \sum_{\alpha} | \alpha JM \rangle \langle \alpha JM | = \frac{2J+1}{8\pi^2} \int d\Omega D^J_{MM}{}^*(\Omega) R(\Omega)$$

We need to calculate the expressions

$$\langle \phi | P^J_M | \phi \rangle = \frac{2J+1}{8\pi^2} \int d\Omega D^J_{MM}{}^*(\Omega) \langle \phi | R(\Omega) | \phi \rangle$$

$$\langle \phi | H P^J_M | \phi \rangle = \frac{2J+1}{8\pi^2} \int d\Omega D^J_{MM}{}^*(\Omega) \langle \phi | H R(\Omega) | \phi \rangle$$

Appendix

If $|\phi\rangle$ is axially symmetric, $J_z|\phi\rangle = M|\phi\rangle$

$$\langle\phi|R(\Omega)|\phi\rangle = e^{-i\alpha M}\langle\phi|e^{-i\beta J_y}|\phi\rangle e^{-i\gamma M}$$

$$D^J_{MM}(\Omega) = e^{-i\alpha M}\langle JM|e^{-i\beta J_y}|JM\rangle e^{-i\gamma M}$$

then, using the "reduced rotation matrix" $d^J_{MM'}(\theta) = \langle JM|e^{-i\theta J_y}|JM'\rangle$

$$\langle\phi|P^J_M|\phi\rangle = \frac{2J+1}{2}\int_0^\pi d\theta \sin\theta d^J_{MM}(\theta)\langle\phi|e^{-i\theta J_y}|\phi\rangle$$

$$\langle\phi|HP^J_M|\phi\rangle = \frac{2J+1}{2}\int_0^\pi d\theta \sin\theta d^J_{MM}(\theta)\langle\phi|He^{-i\theta J_y}|\phi\rangle$$

$\langle\phi|e^{-i\theta J_y}|\phi\rangle$
- ≈ 1 for $\theta \ll 1$,
- decreases quickly as $\theta \to$ larger ,
- is symmetric about $\theta = \pi/2$.